Clim Dyn (2012) 38:2167–2190
DOI 10.1007/s00382-011-1096-z

Dependence of Indian monsoon rainfall on moisture fluxes across the Arabian Sea and the impact of coupled model sea surface temperature biases

Richard C. Levine · Andrew G. Turner

Received: 14 January 2011 / Accepted: 7 May 2011 / Published online: 24 May 2011

Abstract The Arabian Sea is an important moisture source for Indian monsoon rainfall. The skill of climate models in simulating the monsoon and its variability varies widely, while Arabian Sea cold sea surface temperature (SST) biases are common in coupled models and may therefore influence the monsoon and its sensitivity to climate change. We examine the relationship between monsoon rainfall, moisture fluxes and Arabian Sea SST in observations and climate model simulations. Observational analysis shows strong monsoons depend on moisture fluxes across the Arabian Sea, however detecting consistent signals with contemporaneous summer SST anomalies is complicated in the observed system by air/sea coupling and large-scale induced variability such as the El Niño-Southern Oscillation feeding back onto the monsoon through development of the Somali Jet. Comparison of HadGEM3 coupled and atmosphere-only configurations suggests coupled model cold SST biases significantly reduce monsoon rainfall. Idealised atmosphere-only experiments show that the weakened monsoon can be mainly attributed to systematic Arabian Sea cold SST biases during summer and their impact on the monsoon-moisture relationship. The impact of large cold SST biases on atmospheric moisture content over the Arabian Sea, and also the subsequent reduced latent heat release over India, dominates over any enhancement in the land-sea temperature gradient and results in changes to the mean state. We hypothesize that a cold base state will result in underestimation of the impact of larger projected Arabian Sea SST changes in future climate, suggesting that Arabian Sea biases should be a clear target for model development.

Keywords Indian monsoon · Moisture fluxes · Climate model · Arabian Sea · Model systematic error

R. C. Levine (✉)
Met Office Hadley Centre, FitzRoy Road, Exeter, Devon EX1 3PB, UK
e-mail: richard.levine@metoffice.gov.uk

A. G. Turner
NCAS-Climate, Department of Meteorology, University of Reading, Earley Gate, Reading RG6 6BB, UK

1 Introduction

Changes in northern Indian Ocean sea surface temperatures (SSTs) have the potential to affect monsoon rainfall by altering the amount of moisture available for transport towards India. This is especially the case for the Arabian Sea, where local convective activity is limited to the south eastern part, and any changes in moisture availability will be directly transported towards the Indian subcontinent. Indeed, Gimeno et al. (2010) have shown the Arabian Sea to be an important moisture source for Indian monsoon rainfall. Summer SST variability has the greatest potential to affect monsoon rainfall via a direct impact on moisture fluxes, however previous observational studies show little sign of this, as discussed below. The relationship between concurrent northern Indian Ocean SSTs and monsoon rainfall is complicated by the compensating impacts of SST on the availability of moisture and on the meridional temperature gradient driving the large-scale monsoon flow (e.g. Chung and Ramanathan 2006). Furthermore, due to the strong air-sea coupling over the Arabian Sea and equatorial Indian Ocean, SSTs vary greatly in response to dynamical changes associated with variations in the strength of the Indian monsoon, which are determined largely by external factors such as the El Niño-Southern Oscillation (ENSO) via anomalies to the Walker

Circulation (as first described by Walker 1925). This significantly complicates the detection of monsoon variability related to other changes in the lower boundary of the atmosphere in the global coupled atmosphere–ocean system during summer.

The purported recent weakening of the ENSO-monsoon teleconnection (e.g. Krishna Kumar et al. 1999)—if not simply the result of noise (Gershunov et al. 2001, van Oldenborgh and Burgers 2005)—or indeed any changes to ENSO variability may provide the potential for enhanced impact of local Indian Ocean variability on the Indian monsoon. This can arise, for example, due to the Indian Ocean Dipole (Saji et al. 1999; Ashok et al. 2004) or changes in ocean upwelling along the Somali and Oman coasts (Izumo et al. 2008). At the same time, rapid warming of the Indian Ocean has been observed in recent decades (e.g. Alory et al. 2007), and Indian Ocean warming is projected to continue in a range of 21st century climate scenarios (Meehl et al. 2007). Therefore understanding the monsoon-moisture relationship, and its dependence on SST, and correctly representing this in climate models is important in order to enable us to have confidence in future climate projections of the Indian monsoon. In this study we aim to add to current knowledge of the relationship between monsoon variability and changes in moisture fluxes and local Indian Ocean SST through observational analysis and climate model simulations. A major goal of this study is to address the impact of systematic coupled model SST biases on the ability of models to represent the monsoon and the moisture-monsoon relationship.

The potential for Arabian Sea SST changes to affect Indian monsoon rainfall has previously been shown in various observational and modelling studies. Cold Arabian Sea SSTs were shown to reduce Indian monsoon rainfall via a reduction in moisture transport for the first time in atmosphere-only GCM simulations by Shukla (1975), who investigated the impact of cold SST anomalies centred along the Somali coast ocean upwelling region. However, Washington et al. (1977) presented modelling results showing SST anomalies in the west and east Arabian Sea having no statistically significant impact on Indian monsoon rainfall. More recently Izumo et al. (2008) have shown an important connection in observations and coupled GCM experiments between the reduced ocean upwelling of cold water in the western Arabian Sea in late spring and an increase in Indian monsoon rainfall over the Western Ghats, which arises due to an increase in moisture transport over the Arabian Sea. This localised impact on western Indian rainfall was also found in a previous observational study by Vecchi and Harrison (2004), who showed that warm SST anomalies during the monsoon onset and early summer over the western Arabian Sea are associated with increased rainfall over the Western Ghats during June and July. A regional modelling study by Singh and Oh (2007) also produces consistent results, with an imposed 0.6°C warming throughout the equatorial and northern Indian Ocean resulting in increased rainfall over the Indian peninsula and reduced rainfall over north-east India.

Anomalies in northern Arabian Sea SSTs can also potentially affect monsoon rainfall. A modelling study by Arpe et al. (1998) shows evidence of a link between these SSTs and Indian monsoon rainfall during July, while also highlighting the teleconnection between the Pacific Ocean and the Arabian Sea, with El Niño conditions found to coincide with warm Arabian Sea SSTs due to feedbacks involving the weakening of the monsoon flow. The Arabian Sea is therefore suggested to have a counteracting impact on the ENSO-monsoon teleconnection. The northern Arabian Sea was also found to be important in an observational study by Clark et al. (2000), who noted strong correlations for monsoon rainfall in the 1945–1994 period with SSTs in a small region of the northern Arabian Sea. Clark et al. (2000) also showed that stronger correlations exist with seasonal mean Indian summer monsoon rainfall when using winter and spring SSTs rather than summer SSTs. That study therefore suggests an impact of the SST anomalies through a delayed coupled ocean–atmosphere process, such as that suggested by Webster et al. (1999), rather than via a direct impact on Arabian Sea moisture supply. However, Vecchi and Harrison (2004) are unable to reproduce these results using a different observational SST dataset (NCEP instead of HadISST) and argue that this is due to the relatively small inter-annual variability in the Arabian Sea and the large uncertainty related to the relative lack of observations and the large intra-seasonal variability in the northern Indian Ocean. Other regions, such as the south east Arabian Sea, are also found to have significant correlations with monsoon rainfall (Rao and Goswami 1988), with March–April SSTs positively correlated with June–September monsoon rainfall. However SSTs during the monsoon season have only limited correlations with Indian rainfall, except in summer between western Arabian Sea SST and Western Ghats rainfall, at least since the 1980s (Vecchi and Harrison 2004, Izumo et al. 2008).

Previous studies have shown that Arabian Sea SST clearly has potential to affect monsoon rainfall, although there is variation in the precise impact due to different areas, seasons, observations and models being examined. Here we are interested in changes over the entire Arabian Sea immediately prior to and during the monsoon season, as this whole region will affect moisture fluxes towards the Indian subcontinent. This relationship is particularly of interest as coupled models show varying skill in simulating the monsoon (e.g. Annamalai et al. 2007), while the partially land-enclosed areas of the northern Indian Ocean

provide particular problems, with SST biases covering the whole Arabian Sea common in many coupled models (Marathayil et al. in preparation; also seen in Rajeevan and Nanjundiah 2009, Fig. 10). Such biases have been a long standing problem in the coupled ocean–atmosphere configuration of the Met Office Unified Model (MetUM), with a large cold SST bias especially in winter and spring in the Arabian Sea (see Turner et al. 2005, Fig. 5 for a depiction in a much older model version), accompanied by a smaller cold bias centred in the northern Bay of Bengal.

In Sect. 2 we describe the model and methods used in this study. In Sect. 3 some large-scale aspects of the relationship in the observed system between monsoon variability, moisture fluxes and Indian Ocean SST are examined. In Sect. 4 we show results of monsoon simulations in atmosphere-only and coupled configurations of HadGEM3, a development configuration of the MetUM, and discuss mean climatic biases. In Sect. 5 the results of idealised experiments are described. These are designed to study the role of individual components of coupled model SST biases on the monsoon and the monsoon-moisture relationship. In Sect. 6 we draw conclusions and discuss the implications of this work for future predictions of changes to the monsoon.

2 Materials and methods

In this section we describe the model framework used in this study and the data used in the observational part of the work.

2.1 Observational data

For SST, AMIP-II data (Taylor et al. 2000) for the 1979–1998 period, the HadISST dataset (Rayner et al. 2003) covering 1871–2008, the uninterpolated HadSST2 dataset (Rayner et al. 2006), and the NOAA OI daily SST dataset (Reynolds et al. 2007) covering 1982–2008 are used in the observational analysis and model-observations comparison. For the HadSST2 dataset, which includes a more accurate representation of the limited observations utilised in its production, we use the 5° gridded version (Rayner et al. 2006), which includes a 1961–1990 climatology and anomalies for the 1850-present period.

Indian monsoon rainfall for June to September is taken from the IITM All-India Rainfall dataset (Parthasarathy et al. 1995) for the period 1871–2008. In addition, the IMD one-degree gridded daily rainfall dataset (Rajeevan et al. 2006), constructed from interpolation of 2140 gauge stations since 1951, is used to examine spatial variations in rainfall signals over India. Moisture fluxes are taken from the ERA40 re-analysis for 1958–2001 (Uppala et al. 2005). For rainfall comparison between model and observations we also use GPCP observations from the 2.5° × 2.5° horizontal resolution Version-2 Analysis dataset (Adler et al. 2003), CPC Merged Analysis of Precipitation (CMAP) observations at 2.5° × 2.5° horizontal resolution (Xie and Arkin 1996), and Tropical Rainfall Measuring Mission (TRMM) observations (Kummerow et al. 2000), specifically the 0.25° × 0.25° horizontal resolution merged 3B43 dataset (available from http://daac.gsfc.nasa.gov).

2.2 HadGEM3 climate model description

We use coupled atmosphere–ocean and atmosphere-only configurations of a development version of the MetUM (HadGEM3) in climate mode, similar to the version of HadGEM3 used by Hewitt et al. (2010) and Arribas et al. (2010). The atmospheric resolution is 1.875° longitude by 1.25° latitude, with 38 levels in the vertical. The ocean is solved on an ORCA tripolar grid (Madec 2008) at nominal 1° horizontal resolution, with higher resolution in the tropics (up to 1/3°) for improved representation of tropical waves, and 42 levels in the vertical. The mixing scheme in NEMO has been set to have no interior penetration of turbulent kinetic energy due to surface wave breaking, which notably reduces cold biases at the surface of the northern Indian Ocean. However, as we shall show, cold biases are still present in this region.

Specific changes that have an impact on the model simulation of the Indian summer monsoon compared to HadGEM1 (Martin et al. 2006) are the inclusion of a new prognostic cloud scheme (PC2: Wilson et al. 2008), the inclusion of adaptive detrainment in the convection scheme (Derbyshire et al. submitted), the change from relative humidity dependent Convective Available Potential Energy (CAPE) buoyancy closure to vertical velocity dependent CAPE closure, and an increase in the CAPE closure time-scale from one to 2 h. Both relative humidity and vertical velocity dependent CAPE closure are designed to reduce the CAPE closure time-step when grid-scale convection appears imminent, however the vertical velocity dependent CAPE closure is much more selective than that of relative humidity based closure and allows the baseline 2 h time-scale to be applied almost everywhere. Ultimately these changes result in a significant reduction in the tendency for excessive intermittent convection at a time-step (30 min) level. In terms of the monsoon simulation this reduces excessive convection over the west equatorial Indian Ocean and subsequently enhances the relatively weak convection over the Indian peninsula.

Other changes that have an impact on the monsoon simulation include smoothed forced adaptive detrainment, which is the vertical smoothing of the temperature and humidity increments from the forced detrainment scheme,

resulting in less noise in the temperature and humidity profiles and reduced model rainfall biases over the Indian region. There is also the inclusion of an improved coastal tiling scheme, which treats coastal points as proportionally land and sea, allowing the ocean part to take surface wind speeds from neighbouring ocean points, thus reducing the bias in stress and surface flux calculations (Strachan 2007). This improves rainfall over the Maritime Continent and reduces the model biases over the Indian area. Critical water content for convective precipitation has been made a function of cloud depth, allowing larger water content for shallower clouds, which reduces a persistent wet bias over the Himalayan foothills.

Overall these changes improve the Indian summer monsoon simulation compared to HadGEM1 (Martin et al. 2006) in both atmosphere-only and coupled configurations. The biases in HadGEM3 are discussed in greater detail in Sect. 4. The coupled model is run for present day conditions for a period of 40 years, of which the last 20 years are analysed allowing for spin-up, although we note that the coupled model signals described in this work are consistent for the entire model run. The atmosphere-only model is run for the 1979–1998 period forced by monthly AMIP-II SSTs (Taylor et al. 2000). This version of the atmosphere-only model is also used for a run examining the impact of SSTs derived from the coupled model on the atmosphere-only model, whereby the atmosphere is forced by monthly-mean coupled model SST and sea-ice fields. This run incorporates the interannual variability of the coupled model, and is run for an 18-year period from the final part of the coupled model control run. The idealised sensitivity experiments that are described in Sect. 5 use the atmosphere-only model with local cold SST anomalies superimposed upon the AMIP-II SST forcing.

3 Impact of observed Indian Ocean SST variability on moisture fluxes and rainfall

We examine the relationship between monsoon rainfall and fluxes of moisture in composites for strong and weak monsoon years of vertically integrated moisture fluxes from the ERA40 re-analysis for 1958–2001. Strong and weak monsoon years are defined as positive (negative) departures of one standard deviation from the mean All India rainfall (AIR) observational record. The years used in the compositing are shown in Table 1. Figure 1 shows the resulting difference composites for each month from May to September, superimposed upon precipitation composites from the IMD one-degree gridded data over the same period. Although there are common features to all months, in particular that strong monsoon years are heavily reliant on moisture fluxes originating from the Arabian Sea and also from the Bay of Bengal once the monsoon becomes established, there is distinct seasonality relating to the development of the Somali Jet. In the rainfall signal, the simultaneous onset over Kerala and north of the head of the Bay of Bengal is noted in May, followed by a more countrywide signal in subsequent months. The pronounced rain shadow over south eastern India is also noted in strong monsoon years, particularly during June and September. This analysis does not differentiate between changes in moisture fluxes being forced by changes to local SST or some external (perhaps dynamic) forcing. However, it does suggest that any isolated cooling of the Arabian Sea or other local SSTs will reduce the moisture supply for monsoon rainfall in the absence of large-scale forcing from elsewhere.

As we are interested in any direct impact of SST on monsoon rainfall via changes to moisture fluxes, we examine the relationship between local Indian Ocean SST and monsoon rainfall. Whilst a detailed analysis of the impacts of Indian Ocean SST variability on monsoon rainfall on interannual timescales is outside the scope of this study (see for example Ashok et al. 2004; Izumo et al. 2008), correlations of HadSST2 SST in the local seas during spring, early and late summer with June to September (JJAS) AIR are shown in Fig. 2 (see Fig. 9a for maps of the domains). These are passed through a 21-year sliding window. The Arabian Sea domain covers the entire region (sea-area within 7.5–30°N and 40–80°E), and therefore will include variability from a range of sources. We are interested in this large area as the entire region will affect moisture fluxes towards the Indian subcontinent, while the whole region is also affected by a coupled model cold bias, as we shall show in Sect. 4. In this and the other regional seas, correlations are weak or slightly negative, especially during summer months and in recent decades. Results are similar for western (sea-area within 7.5–15°N and 50–60°E) and eastern (sea-area within 7.5–15°N and 65–80°E) Arabian Sea sub-regions (shown in Fig. 2b, c). Overall this suggests AIR monsoon variability on seasonal timescales is not being forced by contemporaneous SST variability, with the caveat that any local changes over India may be masked by using total AIR. However, in the observed system, SST variability in the regional seas can be a response to several other factors. Firstly, warm SST can result from a weakened Somali Jet via reduced upwelling (c.f. Izumo et al. 2008). Secondly, anomalous subsidence, reduced wind speed and reduced cloud cover resulting from weakened monsoon convection or remote ENSO forcing can increase SST.

In Fig. 3, we show instantaneous correlations between Arabian Sea SST and those elsewhere, demonstrating the strong link between local SST and variability in the East Pacific, also consistent with Arpe et al. (1998). Although this pattern does not look the same as a typical ENSO

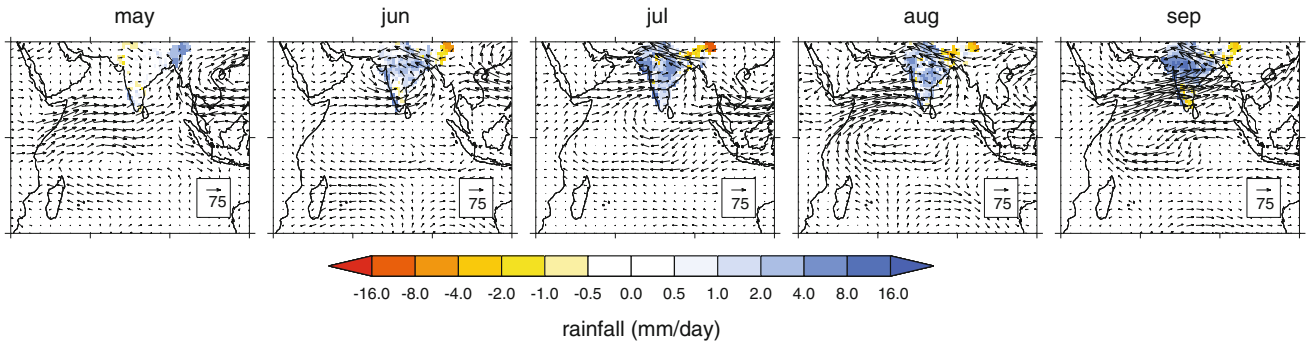

Fig. 1 ERA40 vertically integrated moisture flux anomalies for strong minus weak monsoon composite (determined on basis of years with AIR at least one standard deviation above/below mean, years used are shown in Table 1) for 1958–2001. Monthly means for May–September. Units are kg/m/s. *Contours* show precipitation differences from IMD 1° gridded data (land-only) in mm/day

event, it contains characteristics consistent with ENSO such as the contemporaneous correlations in the eastern half of the basin, centred on the equator, together with correlations of the opposite sign in a horseshoe pattern extending from the equatorial West Pacific polewards to the subtropics. Figure 2 also shows partial correlations between local SST and monsoon rainfall with respect to Niño-3.4 SSTs, a method which removes the linear effects of ENSO. The partial correlations show significant variations through time, with earlier and more recent decades coinciding with a more positive (albeit weak) relationship, especially in the Arabian Sea. The difference between full and partial correlations shows that ENSO has a large impact, which makes the correlations between the Arabian Sea or WEIO and monsoon rainfall more negative. Therefore these SSTs modulate, or are modulated by, monsoon variability driven by ENSO (as suggested by Arpe et al. 1998). The SST-monsoon rainfall relationship is much weaker than that between moisture flux and monsoon rainfall (as shown in Fig. 1). The correlation between June–September mean AIR and the zonal component of June–September mean vertically integrated moisture flux (area-averaged over sea-points of Arabian Sea region as defined in Fig. 2a) is 0.69, which is much higher than the SST-rainfall correlations shown in Fig. 2. Therefore it appears that the Arabian Sea acts mainly to limit the full impact of the ENSO-monsoon teleconnection.

To examine the role of Arabian Sea SST on moisture fluxes more closely, Fig. 4 shows vertically integrated moisture flux anomalies superimposed upon IMD gridded rainfall for India for composites of warm minus cold conditions (using $+1\sigma$ and -1σ deviations respectively, the years used are shown in Table 2). Compositing is performed based on detrended Arabian Sea SSTs north of 7.5°N in DJF, MAM and JJA seasons (Fig. 4 top, middle, bottom respectively) in the HadSST2 data. These figures show large variability throughout the monsoon season. Generally, composites based on boreal winter Arabian Sea SST relate high SST anomalies with increased moisture fluxes incident on the Indian peninsula, similar to the results of Clark et al. (2000) (and perhaps unsurprising due to the use of a similar SST dataset). Additional calculations (not shown) using partial correlations with respect to Nino3.4 DJF SSTs suggest this apparent relationship is not dependent on ENSO. This analysis suggests additional moistening of the atmosphere prior to the monsoon onset. Moving through spring to the JJA composites however, the opposite picture is generally observed. In the early monsoon season there is a reduction in transport from the Arabian Sea towards India in warm years. This is probably due to either a weakening of the meridional temperature gradient necessary for monsoon onset (Li and Yanai 1996), or a reaction to simultaneous warming in the equatorial Pacific (an El Niño signal, as suggested in Fig. 3). Warm Arabian Sea SST anomalies in JJA may themselves be the result of delayed monsoon onset and thus consistent with north-easterly wind anomalies and reduced upwelling of cold water in the western Arabian Sea. In July this signal reverses briefly as the monsoon jet feeds directly into the monsoon trough region, setting off a positive feedback due to increased moisture availability from the Arabian Sea. In September, when the climatological land-sea temperature contrast has already begun to recede and the monsoon is instead maintained by its own latent heat release (Sperber et al. 2000; Holton 1992), higher temperatures bring additional moisture to the monsoon.

We note that the rainfall anomalies in Fig. 4 show evidence of regional rainfall differences on an interannual time-scale, which also vary within the monsoon season. Although there is no coherent signal for the JJA composites that is sustained throughout the entire monsoon season, the figure does suggest anomalies over northern India tend to be more negative, while there is some evidence for more positive anomalies over central India. The balance of these two signals is consistent with the overall negative/neutral impact on total AIR, as shown in the correlations between JJA Arabian Sea SST and total AIR in Fig. 2a. The large

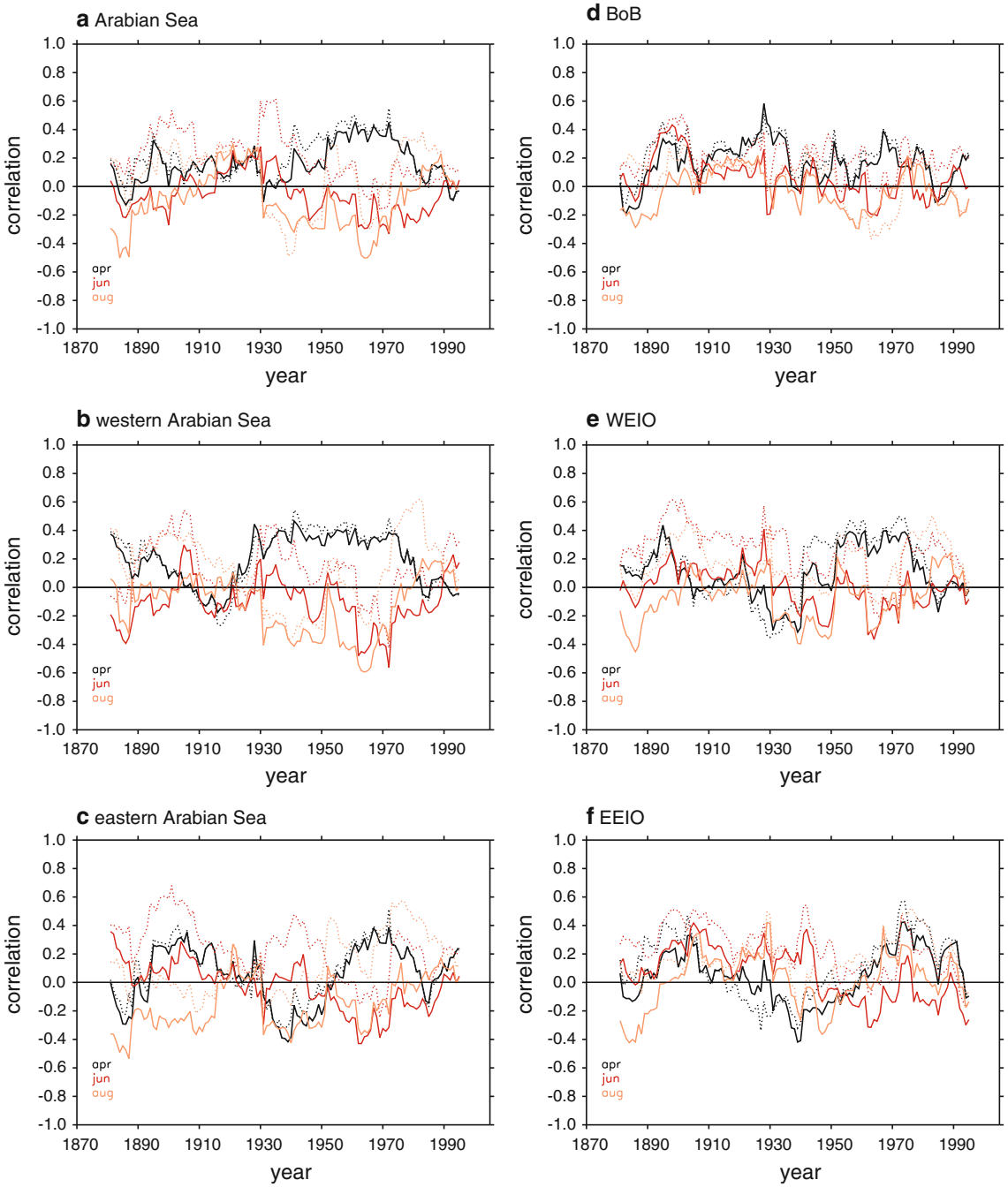

Fig. 2 Observed correlation between seasonal mean (JJAS) AIR and HadSST2 SST in regional seas **a** Arabian Sea (40–80°E, 7.5–30°N), **b** western Arabian Sea (50–60°E, 7.5–15°N), **c** eastern Arabian Sea (65–80°E, 7.5–15°N), **d** Bay of Bengal (80–100°E, 7.5–30°N), **e** WEIO (40–80°E, 15°S–7.5°N), **f** EEIO (80–100°E, 15°S–7.5°N) during late spring (April), early summer (June) and late summer (August) over the 20th century. Partial correlations with respect to contemporaneous Niño-3.4 conditions are shown *dashed*. Correlations are calculated using a 21-year sliding window

area of the Arabian Sea under consideration here possibly masks the impact of variability over smaller regions such as the western Arabian Sea (Vecchi and Harrison 2004, Izumo et al. 2008), although similar versions of Fig. 4 using composites based on western and eastern Arabian Sea (not shown for brevity) result in very similar signals in both moisture fluxes and Indian land rainfall anomalies as when using the full Arabian Sea region.

The impact of summer SSTs is likely to be masked by strong air-sea coupling during summer, which tends to weaken SST anomalies that are present at the start of the monsoon through mixing and evaporation feedbacks and

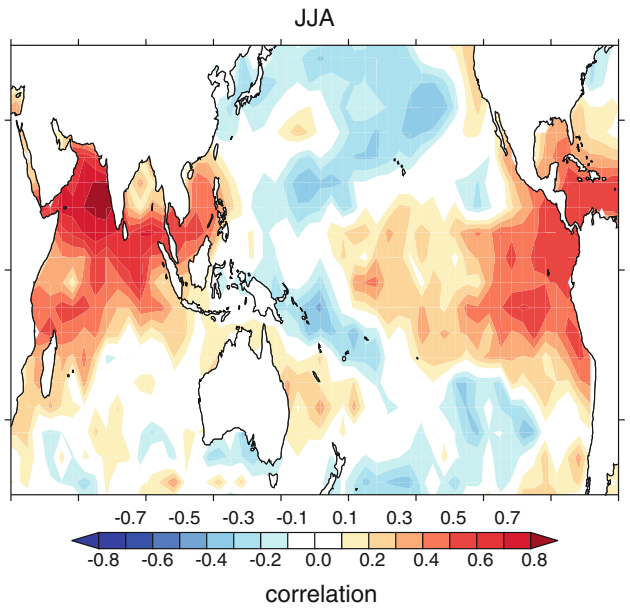

Fig. 3 Instantaneous JJA correlation between Arabian Sea and global SST from the HadSST2 dataset over the 1958–2001 ERA-40 period

coastal upwelling in the case of the western Arabian Sea. Similarly, ENSO variability will only feed back onto the Arabian Sea through the development of the monsoon flow in summer. This will link weak (strong) monsoons to warm (cold) summer Arabian Sea SSTs even if the Arabian Sea SSTs help to modulate the effect of ENSO on the monsoon. This means warm summer SST often implies that there must be less monsoon rainfall and weaker moisture fluxes due to externally forced monsoon variability.

In summary, while clear in-phase relationships can be shown between SST variations in boreal winter/spring and moisture fluxes incident upon India, during the monsoon season itself the effect of observed positive local SST variations on the moisture holding capacity of the atmospheric column is outweighed by reductions in the strength of the meridional temperature contrast and by ENSO. Nonlinear ENSO effects and other external sources of variability may also play a role in the apparent weak SST-rainfall correlations. We note, however, that observed interannual variability in Arabian Sea SSTs (as measured by the standard deviation over the entire Arabian Sea, not shown) is relatively small at only a few tenths of a degree in the HadISST dataset (and slightly larger at around 0.4 K for JJA mean in the NOAA OI daily SST dataset, as we will discuss in more detail in Sect. 4.2), although there are larger local variations in the western Arabian Sea upwelling region. However, SST changes extending over the

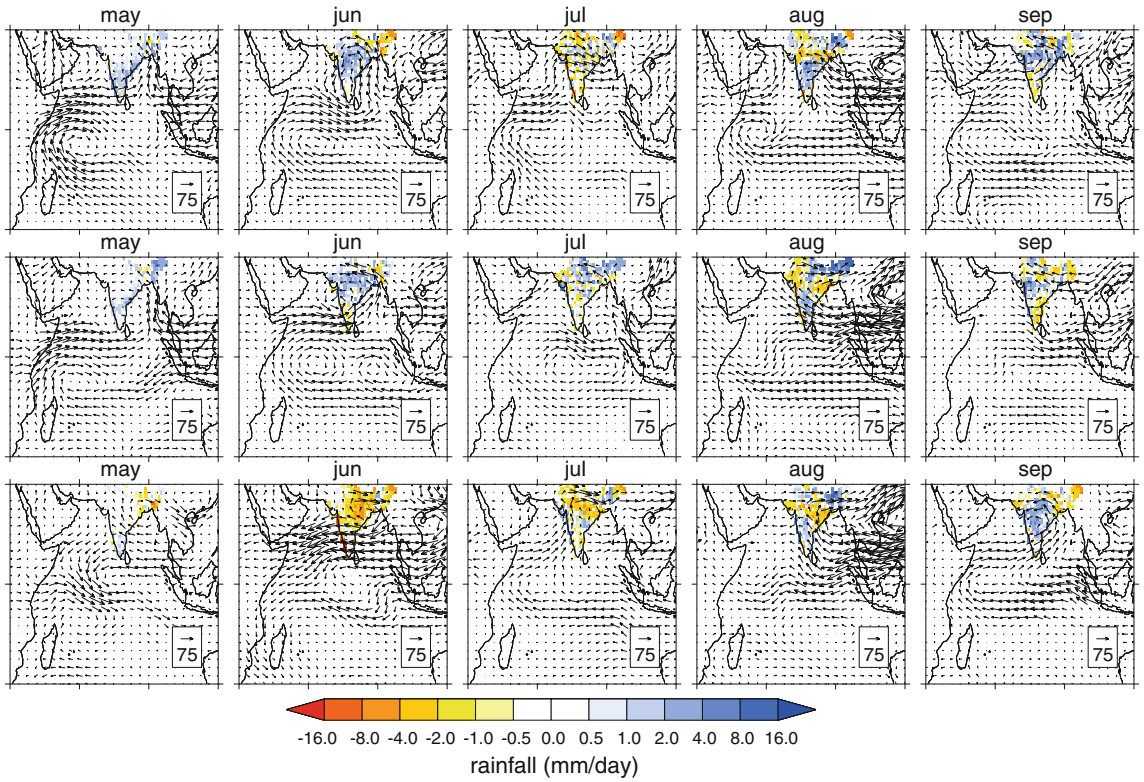

Fig. 4 ERA-40 vertically integrated moisture flux composite differences for strong minus weak SST forcing in the Arabian Sea during DJF (*top*), MAM (*middle*), JJA (*bottom*). Based on a detrended HadSST2 SST over the 1958–2001 ERA-40 period. Units are kg/m/s. *Contours* show precipitation differences from IMD 1° gridded data (land-only) in mm/day. Years used in compositing for Arabian Sea are shown in Table 2

entire Arabian Sea region that may arise due to longer-term climate change or coupled model biases (to be shown in Sect. 4) are very likely much larger than observed interannual variability. Larger SST anomalies will induce far larger changes in evaporation and atmospheric moisture content through the nonlinear Clausius-Clapeyron relationship and thus may allow for a larger impact for local SST on monsoon rainfall.

In the next section we discuss monsoon simulations and biases in the HadGEM3 model.

4 Indian monsoon simulation in HadGEM3

4.1 Climatological monsoon rainfall and winds in atmosphere-only and coupled runs

Figure 5 shows the monsoon seasonal mean climatological 850 hPa wind and precipitation fields for the atmosphere-only and coupled models (anomalies for coupled model are shown only for 95% significance level using an unpaired student t-test). The atmosphere-only control run has reasonably realistic winds in comparison to various re-analysis datasets (not shown), with a small anti-cyclonic bias over India. In terms of precipitation this corresponds to reasonably realistic total all–India rainfall (AIR hereafter), with a JJAS average of 6.5 mm/day (calculated using the mask shown in Fig. 6d) as opposed to 6.9 mm/day and 6.8 mm/day respectively for the long-term 1871–2005 period average and the 1979–1998 AMIP-II period average from the IITM All-India Rainfall dataset. However, there are errors in the spatial distribution of the rainfall, which are shown in Fig. 6a–c. These figures compare the JJAS mean of atmosphere-only model rainfall for 1979–1998 to TRMM observations for 1998–2009. This comparison shows a relative lack of precipitation over central India and over the Western Ghats, an excessive area of inhibited precipitation over the western Bay of Bengal, and enhanced precipitation over the west equatorial Indian Ocean (WEIO) and the Himalayan foothills. Convection tends to be favoured over these latter regions due to the large availability of moisture and heat over the equatorial Indian Ocean and the orographic forcing as the low-level monsoon flow hits the Himalayan foothills respectively. This error pattern has been present in both atmosphere-only and coupled configurations of the MetUM since HadGEM1 (Martin et al. 2006), and the extent and magnitude of the biases are common even amongst the best performing CMIP3 models (e.g. Annamalai et al. 2007; Bollasina and Nigam 2009; Kim et al. 2008).

The basic climatological error is improved in the current atmosphere-only version of HadGEM3, with a reduction of the dry bias over central India compared to HadGEM1. The seasonal cycle of total AIR, despite errors in spatial distribution across the Indian subcontinent, is now also quite realistic. Figure 6e shows the seasonal cycle of AIR for the model compared to TRMM, GPCP, CMAP and IITM observations, highlighting that the atmosphere-only model performs well.

The coupled model shows a large reduction in rainfall over India, the Arabian Sea, Bay of Bengal and equatorial Indian Ocean (Fig. 5c) compared with the atmosphere-only model. AIR is reduced by $71 \pm 8\%$ (95% confidence interval) in the coupled model with respect to the atmosphere-only model mean, with reductions over a large part of India. The error bounds for changes in AIR have been calculated using a student t-test at 95% significance (computed by mean $\pm\, z_{\alpha/2}\, \sigma_D/\sqrt{N}$, where σ_D is standard deviation, N is number of samples, and using $z_{\alpha/2} = 1.96$). The reduction of Indian rainfall in the coupled model can also be seen in the seasonal cycle of AIR (Fig. 6e). The drying signal over India is balanced by an increase in rainfall over the Maritime Continent and West Pacific, with another small increase in the far western equatorial Indian Ocean. The reduced Indian rainfall coincides with reduced cyclonic flow over the monsoon trough area (Fig. 5d) and weakened flow over the Arabian Sea and India. Instead the westerly flow accelerates in the east equatorial Indian Ocean (hereafter EEIO) and southern Bay of Bengal towards the South China Sea and west Pacific Ocean. The interannual variability of AIR in observations has a standard deviation of only around 10%, highlighting the importance of understanding the large 29% reduction of AIR seen in the coupled model.

4.2 Coupled model SST biases

The June–September mean SST biases in the coupled model, with respect to AMIP-II SSTs for the 1979–1998 period, can be seen in Fig. 7a. In general the SST biases are much reduced compared to HadGEM1 (not shown), especially over the north Indian Ocean, although there is now a warm bias in the southern hemisphere. The magnitude and extent of the cold bias across the Pacific has also improved in this version of HadGEM3, with improvements in the representation of ENSO compared to HadGEM1 in terms of Niño-3 SST and Niño-4 wind stress (Martin et al. 2010).

Despite the improvements, cold biases are still present in the north Indian Ocean, with a bias of over -2 K in the Arabian Sea and a smaller bias of around -1 K in the Bay of Bengal. These cold biases also extend southwards into the equatorial Indian Ocean. These biases have been a long-standing problem in the MetUM. Indeed other derivatives of the MetUM, such as HiGEM (Shaffrey et al. 2009), have similar cold biases caused by similar mechanisms, which are described in detail by Marathayil et al.

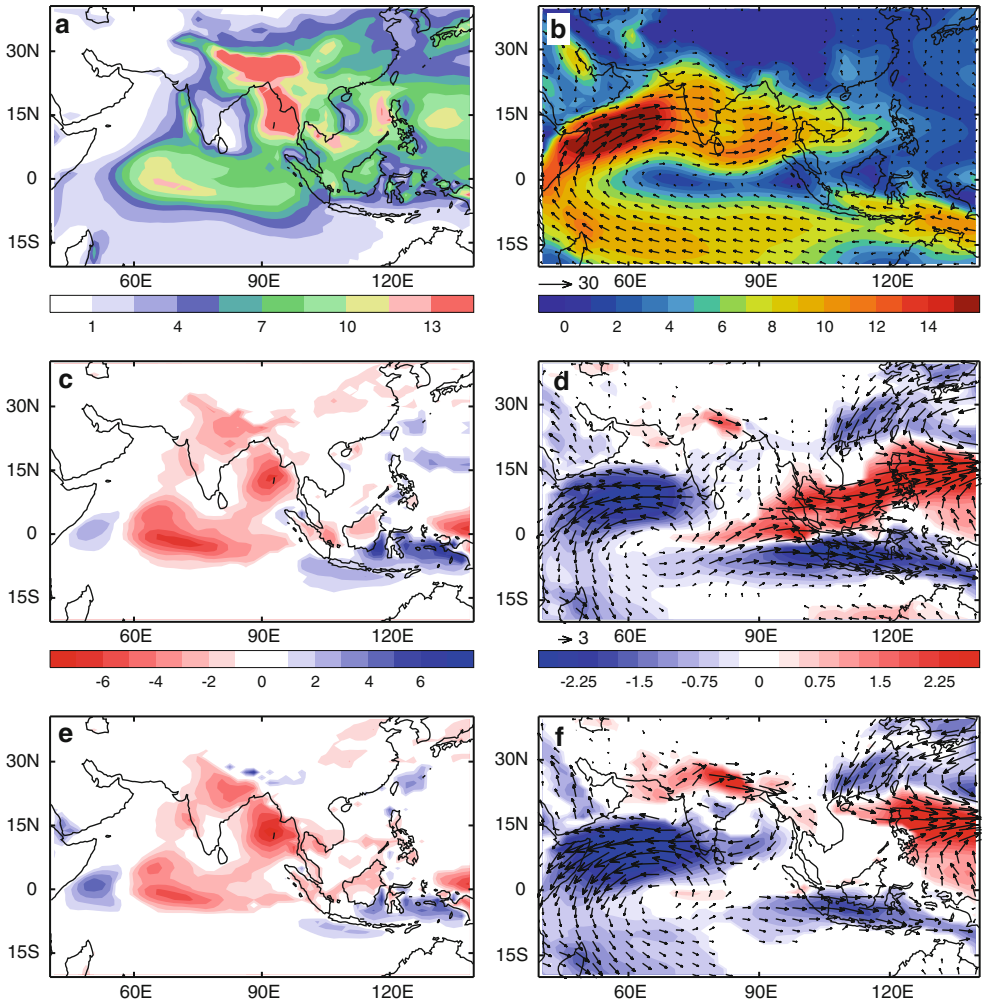

Fig. 5 Atmosphere-only model (control) June–September mean **a** precipitation, **b** 850 hPa winds; Coupled model difference with control, **c** precipitation anomalies, **d** 850 hPa wind anomalies; Atmosphere-only model forced by coupled model SSTs difference with control, **e** precipitation anomalies, **f** 850 hPa wind anomalies. Units for precipitation and winds are mm/day and m/s respectively. *Anomalies* are only shown for signals significant at 95% level using a student t-test

(in preparation). The cold biases develop in winter, and are linked to excessive latent heat fluxes and strong low-level north-easterly flow over the Arabian Sea. These excessive wind stresses result in excessive mixing in the ocean and the development of an anomalously thick mixed layer, which persists until summer and significantly limits temperature variability at the surface. The mixed layer depth in the Arabian Sea in HadGEM3 does still show a reasonable seasonal cycle compared to the observed climatology from de Boyer Montégut et al. (2004), although the timing of the minimum in the mixed layer depth, which in observations occurs in March–April, is delayed by approximately a month in the model. The likely mechanism contributing towards the strong wind stresses include year-round persistent precipitation biases over the western equatorial Indian Ocean. This excessive equatorial convection results in enhanced low-level convergence drawing in air from the continent surrounding the Arabian Sea. Furthermore, a cold surface air temperature bias to the north and north-east of the Arabian Sea in winter enhances the meridional pressure gradient and produces strong flow over the Arabian Sea. The excessive Arabian Sea wind stresses, and the related excessive equatorial rainfall bias and continental cold temperature bias, are also present in the atmosphere-only model. This suggests that the error originates in the atmosphere.

The excessive rainfall over the tropical Indian Ocean, which is one of the causes of the strong winter Arabian Sea wind stress and subsequently leads to cold Arabian Sea SST, is common amongst many models (e.g. Bollasina and Nigam 2009). As discussed in Sect. 4.1 this excessive equatorial Indian Ocean rainfall appears to be an inherent feature of the MetUM convection scheme, with preferential model convection over areas with large amounts of

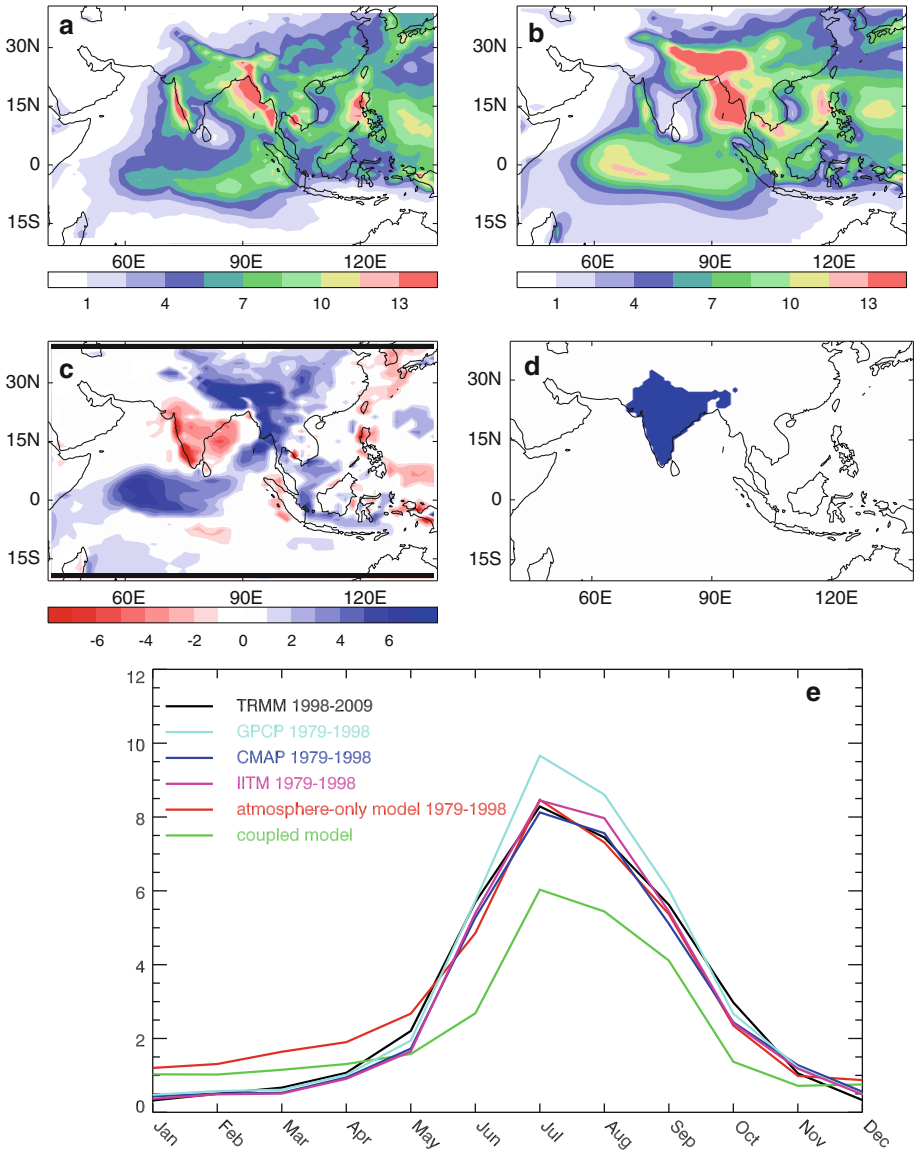

Fig. 6 Precipitation (mm/day) for **a** TRMM observations: 1998–2009, **b** atmosphere-only model: 1979–1998. **c** precipitation anomalies (mm/day) for atmosphere-only model minus TRMM (anomalies are only shown for signals significant at 95% level using a student t-test). **d** *Mask* used for calculating all-India rainfall. **e** Seasonal cycle of AIR for atmosphere-only and coupled model versus TRMM, GPCP, CMAP and IITM observations

available heat and moisture. This bias appears in shorter time-scale forecasts as well as climate runs of the MetUM, and is consistent with errors in the distribution of tropical diabatic heating (Martin et al. 2010). The magnitude of the wet bias over the equatorial Indian Ocean (and subsequently the magnitude of the summer dry bias over central India) is sensitive to parameter settings in the convection scheme, such as entrainment and detrainment rates, adaptive detrainment (Derbyshire et al. submitted) and the CAPE time-scale. However, it is often found that further local improvements in the mean state over the Indian Ocean and Indian subcontinent are accompanied by degradation to the mean state in remote regions and to variability in general. This sensitivity of rainfall in the tropics to changes in convection settings is consistent with findings in other models such as those of Hourdin et al. (2006). In that study the authors show that in the LMDZ4 model large-scale ascent over continents can be enhanced, and strong rainfall over tropical oceans suppressed, as a result of changes in convective heating distribution and the inclusion of precipitating downdraughts.

There is still a cold bias present in the equatorial Pacific Ocean (Fig. 7a), which is related to excessive wind stress and a consequent increase in upwelling of cold water to the surface. The use of high resolution coupled models (1/3° ocean) has been shown to reduce this bias from historical levels by resolving tropical instability waves (e.g. in HiGEM; Shaffrey et al. 2009). This equatorial Pacific cold bias has the potential to affect the monsoon through the Walker circulation. In this paper we will focus on these three biases (Arabian Sea, Bay of Bengal, and equatorial Pacific Ocean), as these are common amongst many

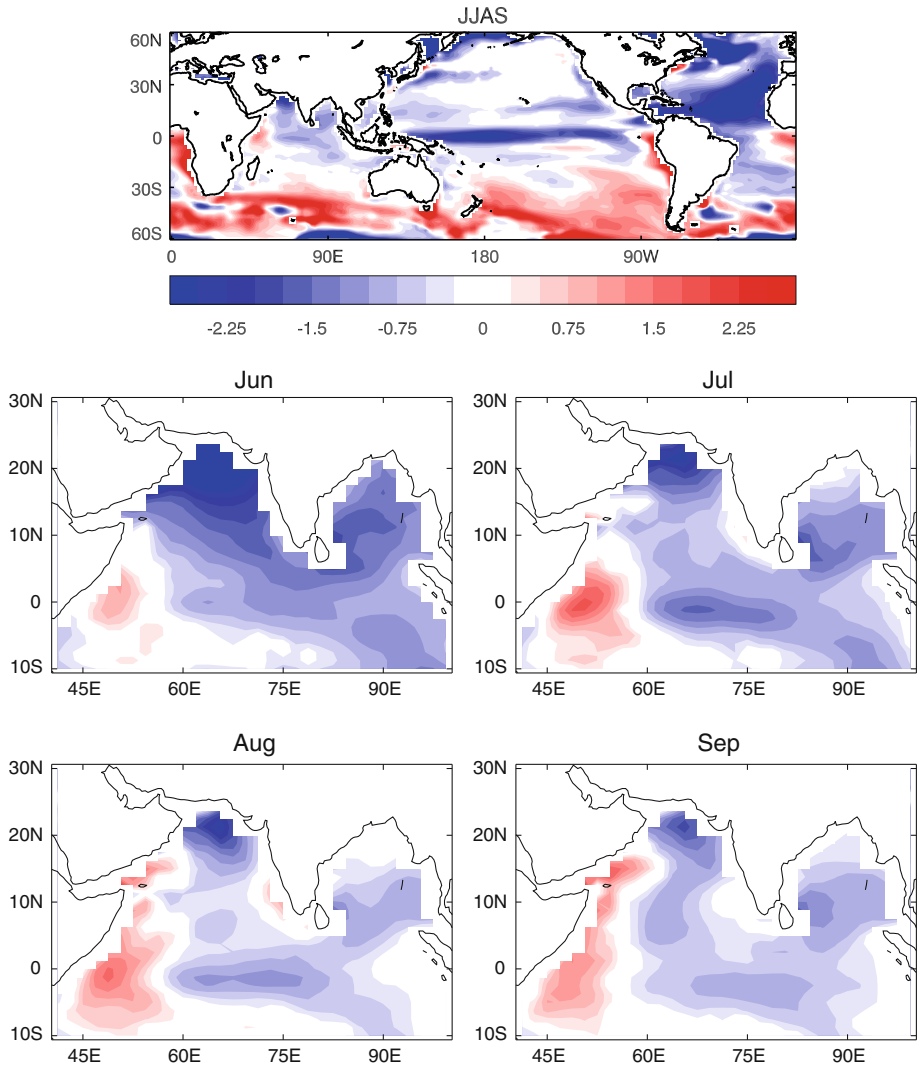

Fig. 7 SST difference (K) between coupled model and AMIP-II SSTs (1979–1998 period for latter): **a** June–September mean, **b** June, **c** July, **d** August, **e** September. Anomalies are only shown for signals significant at 95% level using a student t-test

models (e.g. Lin 2007; Marathayil et al. in preparation), and because we will show that these play a large role in the detrimental impact on Indian monsoon rainfall in the coupled model.

Looking at SST biases in the northern Indian Ocean more closely through the monsoon season, Fig. 7b–e shows that the Arabian Sea bias gradually decreases throughout the season. The cold bias becomes more confined to the northern Arabian Sea, while a warming appears in the western Arabian Sea around the upwelling region along the Somali coast. This local warming may be the result of the weaker low-level atmospheric flow relative to the atmosphere only model (see Fig. 5d), and may act to modulate any negative impact from the surrounding cold SSTs on monsoon rainfall (Izumo et al. 2008).

The annual cycles of AMIP and coupled model SST in the northern Indian Ocean are shown in Fig. 8. These show the changes that occur as a result of the onset and retreat of the monsoon circulation, with significant warming until mid-May in the observations from when the monsoon winds dramatically gain speed, reducing SST there (see Ju and Slingo 1995 for a detailed description). Strong ocean–atmosphere coupling in the Arabian Sea at this time means that the observed interannual variability is relatively small, particularly in areas further away from the upwelling region along the Somali coast, such as the northern Arabian Sea. Using the NOAA OI SST dataset (0.25° × 0.25° horizontal resolution) for the 1982–2008 period (Reynolds et al. 2007), which shows larger interannual variability than HadISST over the Arabian Sea, the interannual standard deviation of SST over the whole Arabian Sea (sea-area within 7.5–30°N, 50–80°E) meaned over JJA and June is 0.37 and 0.46 K respectively. Variability is largest in the upwelling regions of the western Arabian Sea (here averaged over sea-area within 7.5–15°N, 50–60°E), at 0.46 and 0.65 K for JJA and June means respectively, and can locally reach just over 1 K. Lower variability is found in the eastern Arabian Sea (sea-area within 7.5–15°N,

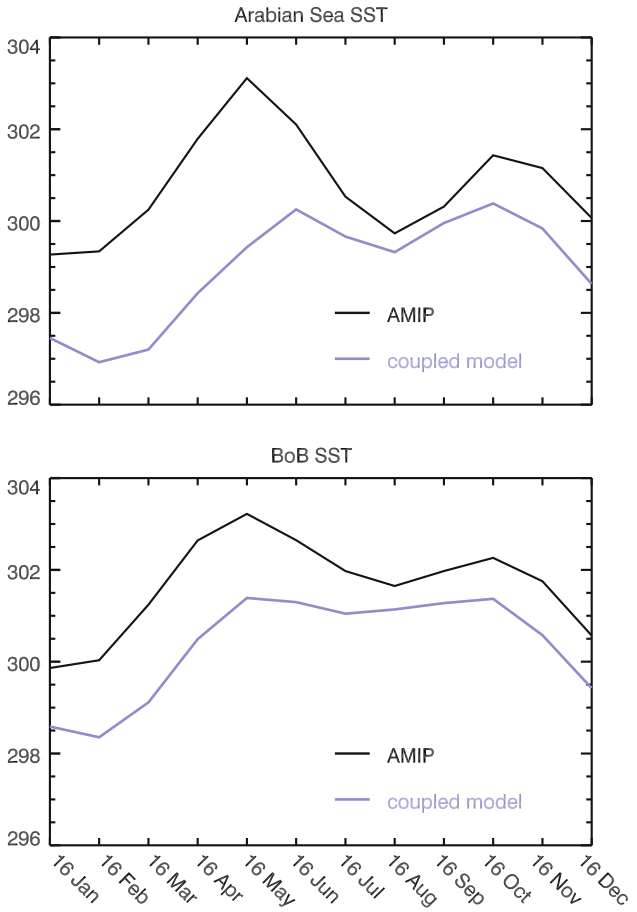

Fig. 8 Annual cycle of SSTs (K) for coupled model and AMIP-II: **a** Arabian Sea (40–80°E, 7.5–30°N), **b** Bay of Bengal (80–100°E, 7.5–30°N)

65–80°E) at 0.38 and 0.50 K for JJA and June means, while variability is lowest in the northern Arabian Sea (sea-area within 20–30°N, 50–80°E) at 0.39 and 0.31 K for JJA and June means.

The observed interannual variations in SST area-averaged over the entire Arabian Sea (0.37 K/0.46 K for JJA/June means) are considerably smaller than the Arabian Sea SST bias in the coupled model (−1.0 K/−1.9 K for JJA/June means). Locally over the northern Arabian Sea the coupled model SST bias reaches over −3 K, which is far greater than observed interannual variability. In the coupled model the cold bias over the southern Arabian Sea starts to reduce after May due to the delayed onset and weakening of the Somali Jet. The development of strong flow (>10 m/s at 850 hPa) over the southern Arabian Sea is delayed by over 3–4 pentads compared to the atmosphere-only model, which allows the coupled model Arabian Sea SST to keep on rising for longer than in observations. The ocean–atmosphere interaction tends to further reduce the cold bias during the monsoon season itself as the reduced strength of the monsoon flow results in reduced surface cooling.

4.3 Biases in an atmosphere-only run forced with coupled model derived SSTs

To understand the impact of the coupled model SST biases on the monsoon we have performed an atmosphere-only run forced by monthly-mean coupled model SSTs and sea-ice fields, as described in Sect. 2. The mean anomalies compared to the atmosphere-only control run (Fig. 5e, f) are very similar to the coupled model anomalies (Fig. 5c, d). AIR is reduced by 29 ± 8% compared to the control run mean, similar to the coupled model bias. The small area of enhanced orographically-forced rainfall over the Himalayan foothills (Fig. 5e) is a typical response of the HadGEM3 atmosphere-only model to reduced rainfall over central India, due to increased divergence of the low-level flow against the Western Ghats as the monsoon jet makes landfall over western India. This results in enhanced flow over northern India and the Himalayan foothills.

The result here suggests that the relatively poor monsoon rainfall in the HadGEM3 coupled model is forced largely by global SST biases. This forcing of the atmosphere by biases in the ocean suggests a role for the direct impact of SST on Arabian Sea moisture availability during spring and/or summer affecting the pre-monsoon and monsoon periods, while the impact of SST biases on the atmosphere during winter is less likely to be sustained within the atmosphere until the summer monsoon season. In contrast to the findings for observational anomalies in Sect. 3, this suggests isolated variations in Arabian Sea SST (such as substantial coupled model biases) might directly affect monsoon rainfall. Previous work (Shukla 1975; Vecchi and Harrison 2004; Izumo et al. 2008) would suggest that this could be due to a cold SST bias in the western Arabian Sea, which could result in reduced rainfall over western India in particular. However, the SST bias in HadGEM3 is more widespread and centred over the northern Arabian Sea, while the cold bias near the Somalia-Yemen-Oman coast reverses at the start of the monsoon season (Fig. 7b). Also, the reduced rainfall in the coupled model compared to the atmosphere-only model occurs over central and northern India as well as western India, thereby indicating a possibly more widespread impact of the coupled model SST biases than earlier studies would suggest.

In the next section we look at idealised sensitivity tests to provide further understanding on the influence of individual local ocean biases on monsoon rainfall and the monsoon-moisture relationship.

5 Idealised experiments studying impact of local SSTs

We present results from a series of atmosphere-only experiments that aim to decompose the impact of the

coupled model SST bias on monsoon rainfall and how the SST bias interacts with, and influences, the monsoon-moisture relationship. The experiments are run for the 1979–1998 period forced by monthly AMIP-II SSTs.

In the first set of experiments we examine the impact of cold anomalies in these areas individually. The coupled model SST bias showed that the model has significant cold errors in the Arabian Sea, the Bay of Bengal, but also in more remote areas such as the equatorial Pacific Ocean (Fig. 7a), and we examine the impact of all these regions separately. Figure 9 shows the patterns of the imposed SST biases in these experiments, and also the annual cycle of the imposed biases in the Arabian Sea and Bay of Bengal. The imposed biases are chosen to reflect the size and pattern of the coupled model biases, and for the Arabian Sea, Bay of Bengal and equatorial Pacific consist of (skewed) Gaussian distributions. The size of the bias averaged over the Arabian Sea is approximately −0.9 K with a maximum of −2 K in the northern part (and hereafter referred to as "north Arabian Sea cold SST experiment"), while the average is −0.55 K over the Bay of Bengal with a maximum of −1 K in the northern part (hereafter referred to as "north Bay of Bengal cold SST experiment"). In comparison with the coupled model Arabian Sea SST bias (Fig. 8) the average magnitude of the imposed bias (−0.9 K) is an underestimate for the first part of the monsoon season. But then the average magnitude of the cold bias in the coupled model is reduced by the warming along the Somali coast upwelling region (Fig. 7e). Therefore in the latter part of the monsoon season, as the coupled model SST bias weakens, the imposed cold SST bias is of similar magnitude to the coupled model bias in the northern Arabian Sea. Over the equatorial Pacific (120–280°E, 10°S–10°N) the average and maximum of the bias are −0.85 K and −2 K respectively. We also consider experiments with cold anomalies over the WEIO and EEIO (−2 K uniform cold anomalies) in order to investigate the sensitivity of the model to SST biases in these areas, which are also important to the Indian Ocean Dipole (IOD) mode (Saji et al. 1999). However, the precise domains are chosen such that we cover the entire north and equatorial Indian Ocean, which is also the area implicated in the coupled model cold SST bias, rather than the traditional IOD regions. We note that the biases chosen for the WEIO and EEIO experiments are larger both than observed interannual variability and coupled model SST biases. The WEIO and EEIO experiments have been designed to qualitatively establish the enhancing or counteracting nature of equatorial biases compared to biases in the northern Indian Ocean. All the biases are smoothed towards the domain edges in order to avoid continuity problems, and are applied for the full year in order to retain the characteristic underlying annual cycle found in the AMIP-II SST forcing dataset.

These idealised atmosphere-only experiments lack the modulating effect of an interactive ocean, which has been suggested to be important towards the latter part of the monsoon season (see Ju and Slingo 1995, and also Sect. 4). We use these experiments to decompose the contributions from different ocean biases to the atmospheric response, with the caveat that the response of the monsoon may be stronger than that in the coupled ocean–atmosphere system. However we also note that lag-1 auto-correlations for monthly Arabian Sea SST in the full 1871–2008 HadSST2 record are large and positive (always 0.71 or above) for all months once the seasonal cycle and the effects of ENSO are

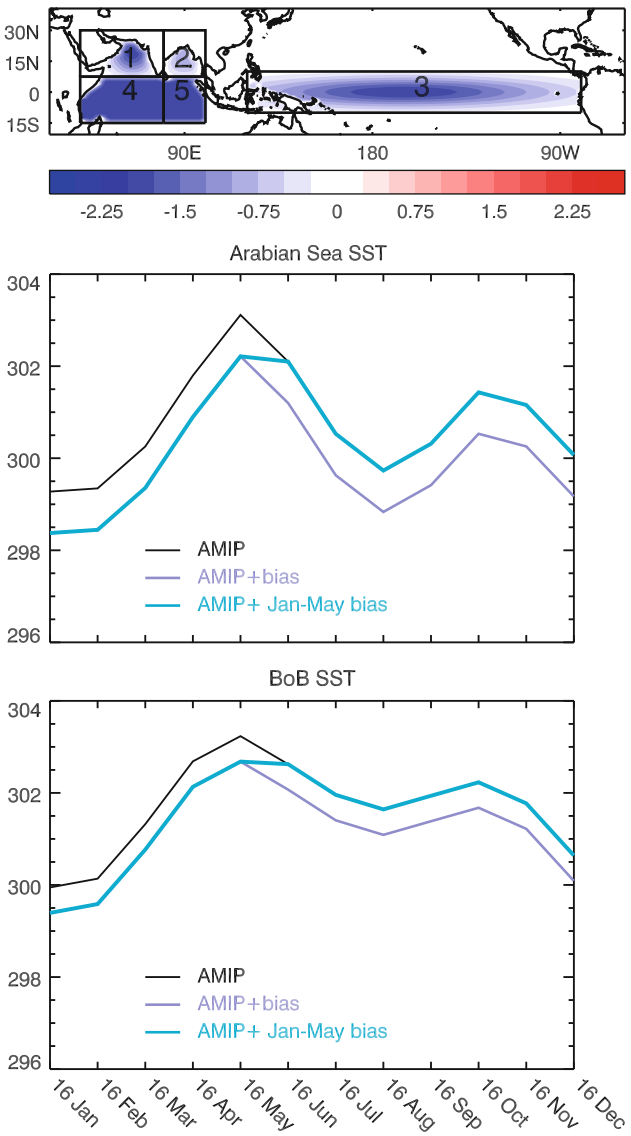

Fig. 9 **a** Areas and SST anomalies (K) applied to AMIP-II SSTs in atmosphere-only experiments: *1* Arabian Sea (40–80°E, 7.5–30°N), *2* Bay of Bengal (80–100°E, 7.5–30°N), *3* equatorial Pacific Ocean (120–280°E, 10°S–10°N), *4* WEIO (40–80°E, 15°S–7.5°N), *5* EEIO (80–100°E, 15°S–7.5°N), **b** annual cycle of applied SST (K) in the Arabian Sea and **c** Bay of Bengal

Table 1 Years (1958–2001 period) used in composites for strong and weak monsoon years in Fig. 1, whereby strong/weak years are determined on the basis of years with AIR at least one standard deviation above/below mean

Strong	1959	1961	1970	1975	1983	1988	1994	
Weak	1965	1966	1972	1974	1979	1982	1986	1987

Table 2 Years (1958–2001 period) used in composites for strong and weak Arabian Sea SST forcing years in Fig. 4, whereby strong/weak forcing years are determined on the basis of years with SST at least one standard deviation above/below mean

DJF strong	1970	1988	1990	1991	1998	1999			
DJF weak	1965	1967	1968	1974	1975	1976	1984		
MAM strong	1969	1970	1977	1980	1988	1998			
MAM weak	1965	1968	1972	1975	1976	1983	1989	1992	1997
JJA strong	1962	1972	1982	1983	1987	1988	1997	1998	
JJA weak	1971	1975	1978	1984	1985	1986	1991	1994	

removed. This suggests that even in the coupled system, Arabian Sea anomalies may be maintained from month to month. We also note that the applied biases (and coupled model biases from which they are derived) are considerably larger than the local interannual variability of SST, and therefore the experimental results are not expected, by design, to provide a realistic representation of interannual variability. Any modulating effect of an interactive ocean that is missing in these experiments is likely to be small. We have already shown using an atmosphere-only run forced by coupled model SST (Sect. 4.3) that the lack of coupled model rainfall is forced largely by SST biases, and therefore that the modulating impact of the ocean in the coupled model is relatively small in the presence of relatively large (compared to interannual variability) SST biases.

5.1 Single Indian Ocean area experiments

Figures 10 and 11 show the impact on precipitation and 850 hPa wind fields for these experiments in terms of June–September means, whereby only the signals at 95% significance levels (using a paired student t-test) are shown. Results in terms of all-India rainfall relative to the atmosphere-only control experiment are listed in Table 3.

5.1.1 North Arabian Sea bias

The north Arabian Sea cold SST bias results in a 22 ± 8% reduction in AIR compared to the atmosphere-only control mean, with reductions over the monsoon trough area and Western Ghats in west peninsular India (Fig. 10a). The precipitation is further reduced over the eastern Arabian Sea, and the Bay of Bengal. This is balanced by small increases over the EEIO and further eastwards over the South China Sea and West Pacific (consistent with Izumo et al. 2008). We note that the dipole between reduced convection over India and increases over the EEIO is similar to that noted during break conditions (e.g., Krishnan et al. 2000).

The 850 hPa winds show that drying over India coincides with weakening of the flow over the entire area covering the Arabian Sea, India and the northern Bay of Bengal (Fig. 11a). Westerly anomalies appear in the EEIO, implying that the westerly flow is strengthened there. In reality this would favour a negative IOD (consistent with Krishnan and Swapna 2009). The westerly flow over the EEIO also increases the cross-equatorial flow. This allows a part of the moisture-laden air over the EEIO to be entrained northwards across the equator into the strong westerly flow towards the South China Sea instead of following the usual pathway into the WEIO and across the equator within the Somali Jet. However, increases in convergence and precipitation occur short of the South China Sea, west of Sumatra. These anomalies in the flow are also present, although stronger, in the coupled model simulation (Fig. 5d). This experiment shows that, if isolated, Arabian Sea SST changes will play a large role in moisture flux and monsoon rainfall variability. In terms of model biases, the reduction of AIR with the north Arabian Sea cold SST bias already explains a large part of the detrimental impact on monsoon rainfall found in the coupled model.

5.1.2 North BoB bias

The north Bay of Bengal cold SST bias results in a smaller impact with only a 6 ± 10% reduction of AIR. However there is some spatial redistribution of the rainfall over the Indian region as shown in Fig. 10b and a strong decrease in convection over the Bay of Bengal. This decrease is the probable cause of the weakened monsoon flow. While there are no noticeable increases in rainfall over the equatorial Indian Ocean itself, the anomalous anti-cyclonic flow over northern India and the northern Bay of Bengal area (Fig. 11b) and small northward shift of rainfall towards the Himalayas is another sign of changes similar to those seen during break conditions (Krishnan et al. 2000), and coincides with the close proximity of the cold SST bias to the monsoon trough formation area.

5.1.3 Equatorial Pacific bias

Next we look at the potential of the cold equatorial Pacific coupled model SST bias to influence the climatological monsoon rainfall. The equatorial Pacific Ocean experiment

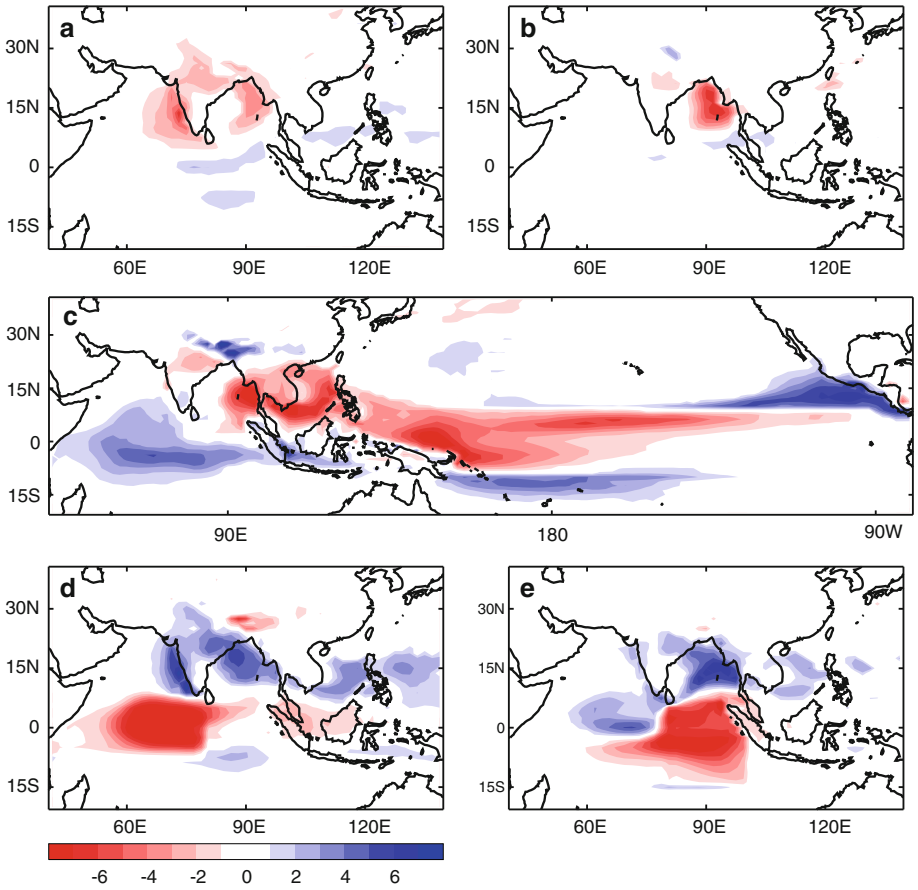

Fig. 10 Impact of idealised anomalies on June–September mean precipitation (mm/day) **a** north Arabian Sea, **b** north Bay of Bengal, **c** equatorial Pacific Ocean, **d** WEIO, **e** EEIO. *Anomalies* are only shown for signals significant at 95% level using a student t-test

does not result in a large change in AIR (2 ± 9% reduction); however the circulation and rainfall over the wider Asian monsoon area are significantly altered. There is a dry signal over central India and the area spanning the eastern Bay of Bengal and the South China Sea, and also over the entire equatorial Pacific, consistent with the reduced SST there. The redistribution of rainfall across the Indian Ocean region results in increased rainfall over the equatorial Indian Ocean, particularly in the western part. This enhances a systematic wet bias in the region inherent to HadGEM3 (Fig. 6c) and other state-of-the-art GCMs (e.g. Annamalai et al. 2007). ENSO variability in the equatorial Pacific has been shown to have a significant impact on the Indian monsoon in various observational and modelling studies (e.g. Webster and Yang 1992, among many others) through modulation of the Walker circulation. However the response found here differs from the typical El Niño-weak monsoon/La Niña-strong monsoon association due to the widespread nature and time-invariance of the imposed SST bias, which covers the West Pacific in addition to the central-eastern regions more commonly associated with ENSO variability. While cold SST anomalies have most in common with La Niña conditions, the drying signal over the Maritime Continent and west Pacific in this experiment paradoxically suggest the model response is more consistent with El Niño conditions. As mentioned previously, this is likely the result of the large spatial extent of the imposed cold bias across the equator.

The consequent impact on the anomalous Walker circulation across the equatorial Indo-Pacific is shown in terms of the velocity potential anomaly at 200 hPa in Fig. 12a. This shows anomalous descent over a large area of the western Pacific, while there is anomalous ascent over the WEIO. This experiment suggests that the equatorial Pacific bias results in a weakening of the development of the monsoon due to inhibition of convection over the West Pacific spreading westwards to the South China Sea and Bay of Bengal, as seen in the monthly evolution of precipitation anomalies in Fig. 12b–f. The westward spread of inhibited convection coincides with a weakening of the low-level westerly flow over the monsoon region. This results in anomalous convergence and convection as the Somali Jet crosses the equator and moves into the Arabian Sea. The westerly monsoon flow over India is significantly weakened in the seasonal mean, especially compared to the previous experiments; however the weakening does not reach the Arabian Sea until August. The delay in the impact over the Arabian Sea appears to be related to

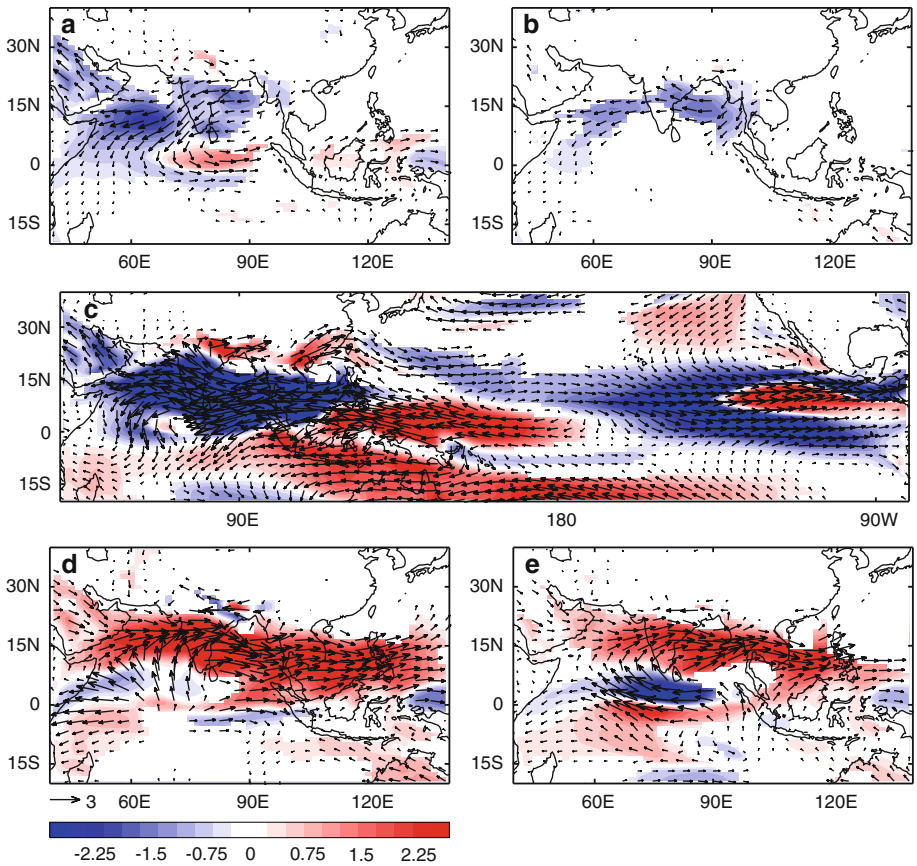

Fig. 11 Impact of idealised anomalies on June–September mean 850 hPa winds (m/s) **a** north Arabian Sea, **b** north Bay of Bengal, **c** equatorial Pacific Ocean, **d** WEIO, **e** EEIO. *Anomalies* are only shown for signals significant at 95% level using a student t-test

Table 3 All Indian rainfall (as % of atmosphere-only control mean) in experiments

	AIR: % of atmosphere-only control run
Experiment results	
(1) atmosphere-only control	100 ± 9
(2) coupled model	71 ± 7
(3) atmosphere-only with coupled model SSTs	71 ± 8
(4) north Arabian Sea	78 ± 8
(5) north Bay of Bengal	94 ± 10
(6) equatorial Pacific Ocean	98 ± 9
(7) west equatorial Indian Ocean	127 ± 9
(8) east equatorial Indian Ocean	114 ± 11
Combinations	
(9) north Arabian Sea + Bay of Bengal	68 ± 6
(10) north Arabian Sea + Bay of Bengal + equatorial Pacific Ocean	69 ± 8
(11) north Arabian Sea + Bay of Bengal: bias applied from January to May only	108 ± 9

95% confidence intervals are calculated using student t-test. All-India rainfall is calculated using a mask of Indian land area at N216 resolution (0.554° latitude by 0.833° longitude), whereby the model data is first interpolated to the higher resolution N216 grid

southeasterly wind anomalies over the Bay of Bengal (Fig. 12c) associated with weakening convection over the Maritime Continent. This initially results in moisture flux anomalies from the Bay of Bengal incident upon north India and local enhancement of Indian rainfall, temporarily limiting the impact of weakening convection over the Maritime Continent on flow over the Arabian Sea. However, this is only sustained through to July, after which the entire low-level monsoon flow across the Arabian Sea, India and the Bay of Bengal weakens. Therefore the main reduction of Indian rainfall only occurs in August and September, and the impact on AIR is further limited by the additional rainfall over the Himalayan foothills, within the AIR area-averaging domain.

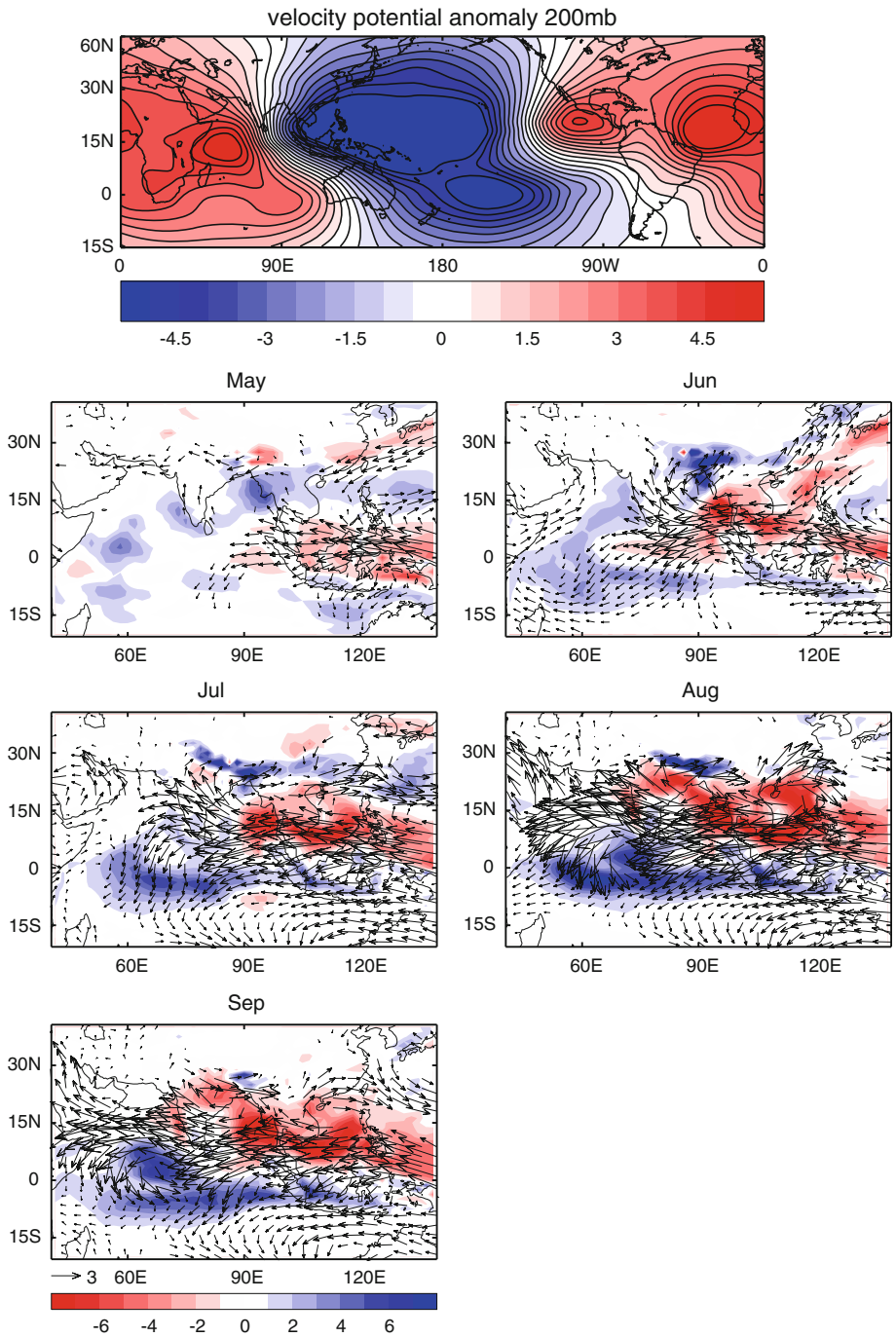

Fig. 12 **a** JJA mean 200 hPa velocity potential anomaly for equatorial Pacific Ocean cold bias experiment—units are 10^6 m^2 s^{-1}, **b–f** May–September monthly mean precipitation anomalies (mm/day) for equatorial Pacific Ocean cold bias experiment, with 850 hPa wind anomalies (m/s) overlaid. *Anomalies* in plots **b–f** are only shown for signals significant at 95% level using a student t-test

The results of this experiment therefore suggest that the impact of the equatorial Pacific bias comes mainly from a direct weakening of convection over the West Pacific, and the subsequent westward shift of convection towards the WEIO. This is confirmed by an additional experiment covering the Maritime Continent only, which results in a similar response (not shown here for brevity). This is equivalent to the results of Soman and Slingo (1997) who found that a warm SST bias over the Indonesia/West Pacific region led to an earlier and stronger monsoon. Additionally, strong increases in convection over the equatorial Indian Ocean may lead to a weakening of the local Hadley circulation. Results from a HadAM3 Maritime Continent warming experiment by Neale and Slingo (2003) are also consistent with the inverse of our equatorial Pacific cold SST experiment in terms of the increase in equatorial Indian Ocean rainfall and the northwards shift in rainfall over India seen in our experiment. Although in Neale and Slingo (2003) this shift in rainfall is seen a bit further east over the Bay of Bengal. The weaker flow from the equatorial Indian Ocean towards the Maritime

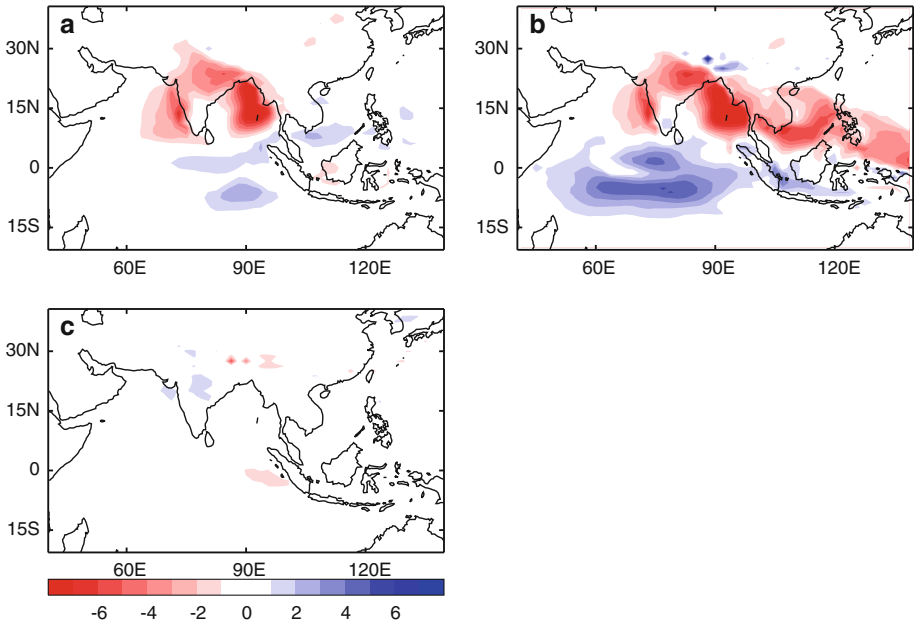

Fig. 13 Impact of additional idealised bias experiments on June–September mean precipitation (mm/day) **a** north Arabian Sea and Bay of Bengal, **b** north Arabian Sea and Bay of Bengal and equatorial Pacific Ocean, **c** north Arabian Sea and Bay of Bengal: bias applied in January–May only. *Anomalies* are only shown for signals significant at 95% level using a student t-test

Continent and stronger flow over north India towards the west Pacific in our experiment is also consistent with the inverse of the experiment by Neale and Slingo (2003). Overall, the impact of the Pacific cold bias on total AIR in our experiment is not as large as that of the local Arabian Sea cold bias, and does not explain the clear detriment to monsoon rainfall sustained through the whole season in the coupled model.

5.1.4 WEIO bias

The WEIO cold bias experiment results in a large 27 ± 9% increase in AIR (Fig. 10d). The rainfall is reduced local to the forcing region and increased further downstream along the pathway of the monsoon jet over the Arabian Sea, India and the Bay of Bengal. This coincides with a huge increase in the strength of the monsoon jet (Fig. 11d). The anomalous model rainfall over the Himalayan foothills is reduced and the monsoon trough intensifies. The increased meridional temperature gradient helps sustain the strengthened monsoon jet throughout the season, ultimately bringing more rainfall to India. The substantial impact in this case may be overestimated because of the presence of excessive precipitation over the WEIO in the atmosphere-only control model, and also to the relatively large imposed SST biases in this case. In terms of coupled model SST biases, this suggests that the extension of the cold SST bias into the equatorial Indian Ocean (increases AIR) provides a compensating impact on the monsoon relative to that of the more northern Indian Ocean cold bias (decreases AIR). We caution however that the lack of a coupled ocean in this framework will prevent the regulating effect of dynamical feedbacks (upwelling, mixing) on the strong monsoon jet and also the cloud impacts on SST.

5.1.5 EEIO bias

The EEIO cold bias experiment results in a smaller 14 ± 11% increase in AIR (Fig. 10e). This experiment reduces rainfall over the local forcing area and results in increases further west over the Indian Ocean, where there is an increase in convergence owing to the anomalous zonal temperature gradient imposed. In observations the developing IOD during June to September is positively correlated with the concurrent Indian summer monsoon rainfall (e.g. Ashok et al. 2004; Izumo et al. 2008). This is consistent with the increased Indian rainfall in the EEIO experiment (similar to a positive IOD event), but not with the results of the earlier WEIO experiment (similar to a negative IOD event), although in the WEIO experiment the imposed SST bias is reducing an existing model bias. So the two effects (model WEIO bias and IOD variability) may cancel each other out, depending on the relative amplitudes and extent of the IOD east and west poles.

5.2 Combined area experiments

In order to determine the overall importance of competing biases, in this section we look at experiments combining areas from the coupled model bias. The results in terms of precipitation anomalies are shown in Fig. 13.

5.2.1 North Arabian Sea and BoB bias

The north Arabian Sea and Bay of Bengal combined cold SST experiment tests the impact of the main local SST bias present in the coupled model. The impact of this combined

Table 4 All Indian Rainfall (as % of atmosphere-only control mean) in additional experiments

	AIR: % of atmosphere-only control run
Experiment results	
(a) north Arabian Sea + BoB: 2× bias	45 ± 5
(b) north Arabian Sea + BoB: 1× bias	64 ± 8
(c) north Arabian Sea + BoB: 0.5× bias	91 ± 9
(d) north Arabian Sea + BoB: 0.25× bias	86 ± 13

95% confidence intervals are calculated using student t-test (here for 1979–1988 period instead of 1979–1998 period for idealised experiments shown in Table 3)

experiment is similar to the sum of the two separate experiments, with AIR equal to 68 ± 6% of the control mean, a close comparison to the 71 ± 8% in the coupled model.

The results for several additional 10-year experiments for the 1979–1988 period that investigate sensitivity to the magnitude of the combined Arabian Sea and Bay of Bengal bias are shown in Table 4. This shows a consistent reduction of AIR for isolated biases in the northern Indian Ocean, which is enhanced as the magnitude of the cold SST bias is increased. The apparent increased impact for the 0.25× bias run (14 ± 13% AIR reduction) compared to the 0.5× bias run (9 ± 9% AIR reduction) is likely the result of atmospheric noise in the relatively short (10-year) runs considered for these additional experiments.

In order to see the impact of the Arabian Sea and Bay of Bengal combined SST bias on the time-mean moisture fluxes we compare the results of the combined Arabian Sea and Bay of Bengal experiment, with observational moisture flux signals shown in Sect. 3. The impact on time-mean precipitation and vertically integrated moisture flux with respect to the atmosphere-only control run is shown in Fig. 14. It shows a clear strengthening of eastward

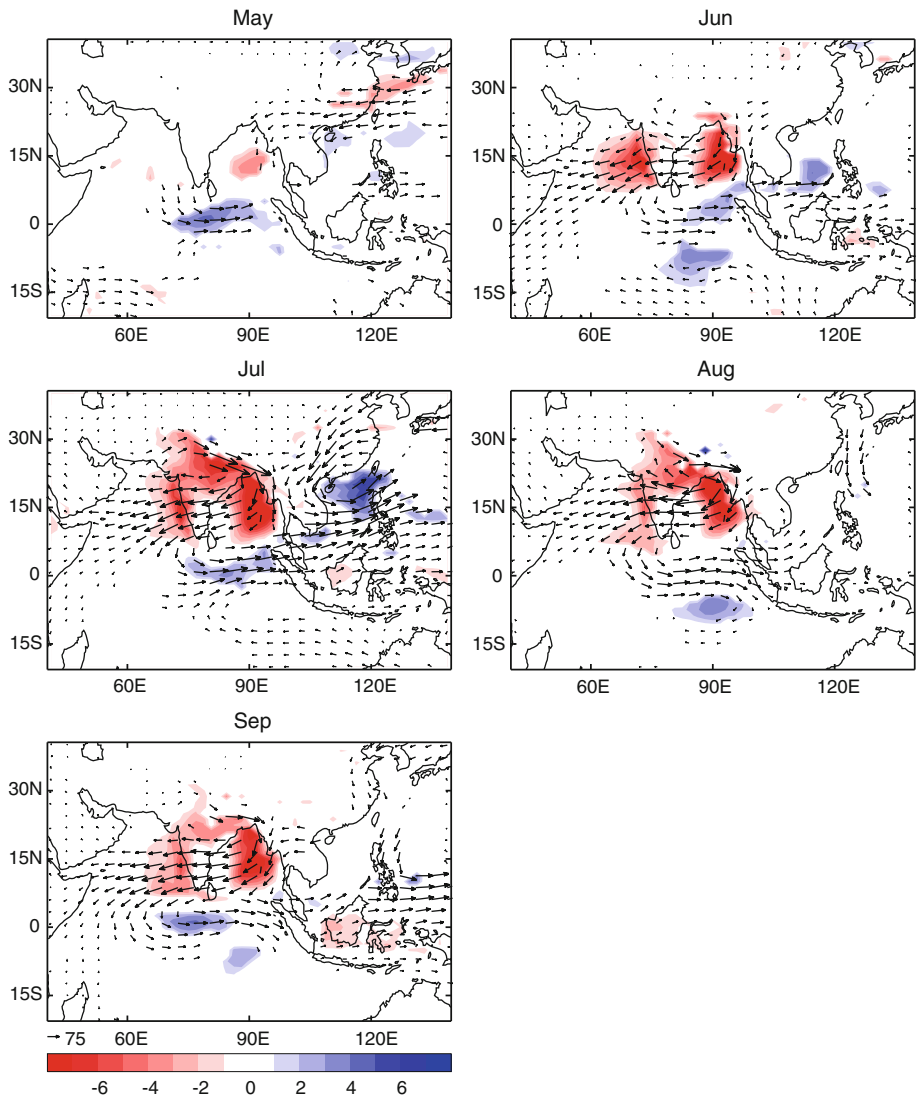

Fig. 14 **a–e** May–September precipitation anomalies (mm/day), with overlaid moisture flux anomaly vectors (kg/m/s) for combined north Arabian Sea and Bay of Bengal cold bias experiment compared to atmosphere-only control. *Anomalies* are only shown for signals significant at 95% level using a student t-test

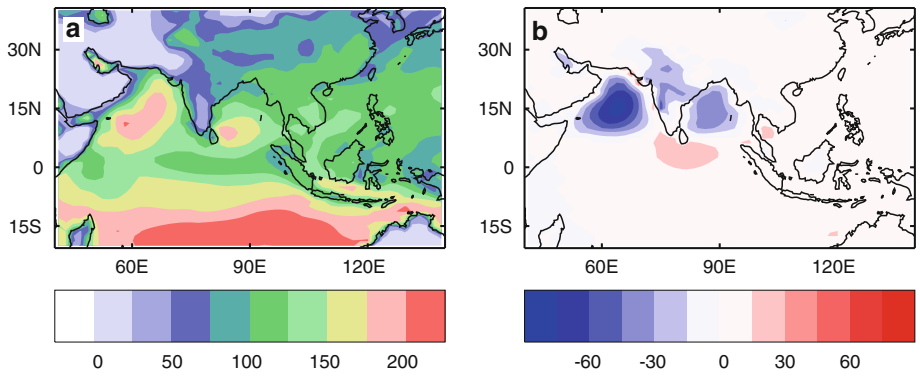

Fig. 15 **a** Surface latent heat flux (W/m^2) averaged over June to September for atmosphere-only model and **b** Surface latent heat flux anomaly (W/m^2) for north Arabian Sea and Bay of Bengal cold SST experiment Anomalies are only shown for signals significant at 95% level using a student t-test

moisture transport towards the EEIO in May, where surface temperatures are highest as a result of the applied cooling further north. This coincides with an increase in rainfall over the equator. The enhanced moisture transport into the EEIO is sustained into the monsoon season, when the expected transport from the Arabian Sea towards India is significantly reduced. Month-to-month variability is much lower once the monsoon has become established. Overall, the moisture flux anomaly fields during the monsoon season are qualitatively similar to the inverse of the ERA40 strong minus weak monsoon year comparison (Fig. 1), again indicating the reliance of strong monsoons on the provision of moisture from the Arabian Sea. We note that the moisture fluxes do not resemble the inverse of the observational moisture flux anomalies composited for warm minus cold Arabian Sea SST years (Fig. 4), given the large impact of external SST signals (e.g. ENSO) in the observed system.

This analysis shows that the local cold SST biases present in the Arabian Sea and Bay of Bengal in the coupled model reduce climatological mean rainfall through weakening of moisture fluxes across the Arabian Sea, via a decrease in evaporation dominating over the impact of the enhanced land-sea temperature gradient. The dominating influence of local evaporation can be seen in the surface latent heat flux anomaly for this experiment in Fig. 15, which shows large reductions in latent heat fluxes over the Arabian Sea. The area-averaged latent heat fluxes over the Arabian Sea are 21 $\pm$ 2% lower (95% confidence interval) than in the atmosphere-only control model. There are also smaller reductions over the Bay of Bengal and India, while there is only little impact further upstream in the monsoon jet over the WEIO and southern hemisphere, showing that reduced monsoon rainfall is directly related to reduced evaporation over the Arabian Sea. The dominating impact of local evaporation on the monsoon over any enhancement of the land-sea temperature gradient is likely a consequence of the nonlinear Clausius-Clapeyron relationship inducing large changes in evaporation and atmospheric moisture content in the case of relatively large SST biases.

5.2.2 North Arabian Sea, BoB and equatorial Pacific bias

Adding the equatorial Pacific cold bias to the Arabian Sea and Bay of Bengal bias is again similar to the sum of the individual impacts, with an increase in rainfall over the WEIO and drying over the area covering the South China Sea to the West Pacific (Fig. 13b). In terms of AIR, there is little change from adding the equatorial Pacific bias (69 $\pm$ 8% of control mean).

Therefore, in terms of the coupled model error in Indian monsoon rainfall the largest contribution comes from the combined Arabian Sea and Bay of Bengal cold biases. The drying over the equatorial Indian Ocean in the coupled model (Fig. 5c) is likely a result of the local southward extension of the cold biases in the northern Indian Ocean to equatorial latitudes, rather than from remote effects, as seen in the local equatorial ocean response to the application of cold biases in the WEIO (Fig. 10d) and EEIO (Fig. 10e). The presence of the cold bias in the equatorial Indian Ocean will also tend to counter any impact from the Pacific bias in the coupled model (comparing Fig. 10d, e with c).

Analysis of lower tropospheric wind anomalies (850 hPa) from the combined experiments (not shown for brevity) suggests a largely linear response to the applied cold biases. Difference maps (not shown) between the impact of combined experiments and the sum of the impacts of the equivalent individual bias experiments show minimal changes for both rainfall and winds, suggesting non-linearities are not significantly affecting the response to combined biases.

5.3 Winter- and spring-time combined Arabian Sea and Bay of Bengal experiment

To examine the sensitivity to the period in which the bias is applied we have performed an additional integration with the combined Arabian Sea and Bay of Bengal cold SST bias applied only for the months of January to May. This gives a further insight into the relative impact of winter/spring versus summer Arabian Sea coupled model SST anomalies.

The results of this experiment reveal a much smaller impact, with an $8 \pm 9\%$ *increase* in AIR. This suggests that the reduction of monsoon rainfall in the experiment with the year-round anomalies is due to the remaining cold SST anomalies in summer. The winter and spring anomalies in observations are suggested to affect the summer monsoon through coupled ocean–atmosphere processes (Webster et al. 1999; Clark et al. 2000), which are missing in the atmosphere-only experiments. However, the strong resemblance of the monsoon simulations in the coupled model and the previously presented atmosphere-only experiments with the combined Arabian Sea and Bay of Bengal anomalies suggests these earlier biases in winter and spring are having little additional impact in terms of monsoon rainfall in the coupled model. This suggests that while small (interannual) north Indian Ocean SST changes may impact the monsoon through coupled processes, larger SST changes (such as coupled model biases) result in moisture changes that dominate over changes in the land-sea temperature gradient due to nonlinearity in the Clausius-Clapeyron relationship. Therefore the impact of these larger SST changes is felt mainly during the summer season itself. The dominance of the impact of reduced evaporation for cold summer Arabian Sea SST biases may also be related to the direct impact of the resulting reduced atmospheric moisture content on the latent heat released during convection over the Indian subcontinent, which is responsible for driving the mature phase of the monsoon (Holton 1992; Sperber et al. 2000).

This result also suggests that larger changes to summer SST may also have potential to directly affect moisture fluxes and monsoon rainfall. Such variations go largely undetected in the observed system owing to a combination of the generally relatively small size of naturally occurring variability in the region and coupled feedbacks that temper their impact on the monsoon, as suggested in Ju and Slingo (1995). As described in Sect. 3, externally forced variability also plays a role given its much larger amplitude.

6 Summary and discussion

We have examined the monsoon-moisture relationship and shown that in observations and the HadGEM3 model strong monsoons are dependent on moisture fluxes across the Arabian Sea. Any link with contemporaneous changes in north Indian Ocean SST is difficult to detect, as also found in previous studies (e.g. Clark et al. 2000), due to air/sea coupling and the strong influence of large-scale induced variability such as ENSO. The processes occurring in the Arabian Sea are important to understand as many coupled models, including HadGEM3, show systematic cold SST biases here (Marathayil et al. in preparation; Rajeevan and Nanjundiah 2009), while state-of-the-art GCMs show varying degrees of skill in simulating the Indian monsoon and its variability (e.g. Annamalai et al. 2007) and problems in reproducing Indian Ocean-monsoon teleconnections (Bollasina and Nigam 2009; Rajeevan and Nanjundiah 2009). Model biases in the north Indian Ocean may therefore influence the sensitivity of the monsoon to climate change as projected by different models.

Analysis of atmosphere-only and coupled model HadGEM3 simulations has shown that global SST biases during the monsoon season force a significant reduction of climatological mean monsoon rainfall over the Indian subcontinent. Using a series of targeted atmosphere-only experiments we can attribute most of this impact on the monsoon to cold SST biases in the Arabian Sea and Bay of Bengal. The biases are found to affect the mean state of the monsoon by weakening the moisture fluxes incident upon India originating from the Arabian Sea. The large impact of the SST biases on the mean state is likely a consequence of the nonlinear nature of the Clausius-Clapeyron relationship, which results in a significant impact on evaporation and atmospheric moisture content over the Arabian Sea. This apparently dominates any competing impact on the land-sea temperature gradient, which in itself may be weak (Chao and Chen 2001). The strong impact of reduced atmospheric moisture content in this case is likely a result of the subsequent reduced latent heat released during convection over the Indian subcontinent, which drives the mature phase of the monsoon (Holton 1992; Sperber et al. 2000). We might also expect the cold base state to affect evaporation and moisture flux variability on interannual and shorter time-scales, however longer model simulations are needed to investigate this.

The impact of the local coupled model SST biases on the mean state comes mainly during the monsoon season, while SST biases imposed prior to the monsoon have almost no impact on the summer monsoon season in atmosphere-only experiments. This shows that the larger correlations in observations between winter and spring Arabian Sea SST and monsoon rainfall must be the result of a coupled process (Webster et al. 1999) or may be partly accidental (e.g. because of ENSO) and may not represent a real cause-effect relationship. However, the similarity between the monsoon simulation in the coupled model, atmosphere-only model forced with coupled model SST and atmosphere-only model with imposed Arabian Sea and Bay of Bengal cold SST bias suggests that relatively large SST anomalies (such as coupled model biases) will impact the monsoon directly during summer due to the dominating impact on moisture through the nonlinear Clausius-Clapeyron relationship. As the Arabian Sea cold SST bias develops in winter due to strong wind stress, persisting into summer through creation of a thick ocean mixed layer (Marathayil et al. in preparation), this means that the impact of the SST bias on the monsoon is itself the result of a delayed coupled process.

This work suggests that relatively large SST anomalies (compared to the magnitude of interannual SST variability) will have a large impact on the monsoon through the monsoon-moisture relationship, and this has potential implications for model sensitivity to future warming of the local Indian Ocean. Model projections for future monsoons indicate generally small positive changes in monsoon rainfall, while models also predict warming of Arabian Sea surface temperatures in the range of approximately +1.5–3.5 K (considering differences between 2080–2099 and 1980–1999 averages in future scenarios SRES A1B, A2 and B1; Figure 10.8 in Meehl et al. 2007), as well as maintaining increases in land-sea temperature gradients (Meehl et al. 2007). These changes in the Arabian Sea are the same order of magnitude as the systematic coupled model SST bias in HadGEM3. From the experiments presented in this study we know that warming of that order of magnitude in the presence of a cold state in the Arabian Sea, which is equivalent to removing the cold bias in the coupled model, would result in a large amount of additional moisture available for monsoon rainfall. However, if such cold biases were removed, due to improved model physics, then we might expect an even greater acceleration of moisture increases due to the nonlinear Clausius-Clapeyron relationship. Therefore we hypothesize that climate models with relatively large cold biases in the Arabian Sea, which are currently relatively common, are potentially underestimating the impact of greenhouse gas forcing and associated surface warming on the monsoon. Similarly any models with warm Arabian Sea SST biases may overestimate increases of monsoon rainfall in future climate scenarios as a result of excessive acceleration of evaporation.

We conclude that it is imperative to understand and improve Arabian Sea biases in coupled models, even if cold (or warm) biases in other models may relate to different processes than those found in HadGEM3, as they may impact monsoon climatology and sensitivity to future climate change.

Acknowledgments Richard Levine was supported by the Joint Department of Energy and Climate Change (DECC) and Department for Environment, Food and Rural Affairs (Defra) Integrated Climate Programme, DECC/Defra (GA01101). Andrew Turner was supported via the National Centre for Atmospheric Science—Climate directorate, a collaborative centre of the Natural Environment Research Council. The authors would like to thank Gill Martin for comments on earlier drafts of the manuscript, and two anonymous reviewers for comments which helped to significantly improve the manuscript.

References

Adler RF et al (2003) The version-2 global precipitation climatology project (GPCP) monthly precipitation analysis (1979–present). J Hydro 4:1147–1167. doi:10.1175/15257541(2003)004<1147:TVGPCP>2.0.CO;2

Alory G, Wijffels S, Meyers G (2007) Observed temperature trends in the Indian Ocean over 1960–1999 and associated mechanisms. Geophys Res Lett 34:L02606. doi:10.1029/2006GL028044

Annamalai H, Hamilton K, Sperber KR (2007) South Asian Summer Monsoon and its relationship with ENSO in the IPCC AR4 simulations. J Clim 20:1071–1092. doi:10.1175/JCLI4035.1

Arpe K, Dümenil L, Giorgetta MA (1998) Variability of the Indian monsoon in the ECHAM3 model: sensitivity to sea surface temperature, soil moisture, and the stratospheric quasi-biennial oscillation. J Clim 11:1837–1858

Ashok K, Guan Z, Saji NH, Yamagata Y (2004) Individual and combined influences of ENSO and the Indian Ocean dipole on the Indian Summer Monsoon. J Clim 17:3141–3155. doi:10.1175/1520-0442

Bollasina M, Nigam S (2009) Indian Ocean SST, evaporation, and precipitation during the South Asian summer monsoon in IPCC-AR4 coupled simulations. Clim Dyn 33:1017–1032. doi:10.1007/s00382-008-0477-4

Chao WC, Chen B (2001) The origin of monsoons. J Atmos Sci 58:3497–3507. doi:10.1175/1520-0469(2001)058<3497:TOOM>2.0.CO;2

Chung CE, Ramanathan V (2006) Weakening of North Indian SST gradients and the monsoon rainfall in India and the Sahel. J Clim 19:2036–2045. doi:10.1175/JCLI3820.1

Clark CO, Cole JE, Webster PJ (2000) Indian Ocean SST and Indian Summer Rainfall: predictive relationships and their decadal variability. J Clim 13:2503–2519

de Boyer Montégut C, Madec G, Fischer AS, Lazar A, Iudicone D (2004) Mixed layer depth over the global ocean: an examination of profile data and a profile-based climatology. J Geophys Res 109(C12003). doi:10.1029/2004JC002378

Gershunov A, Schneider N, Barnett T (2001) Low-frequency modulation of the ENSO–Indian monsoon rainfall relationship: signal or noise? J Clim 14:2486–2492. doi:10.1175/1520-0442(2001)014

Gimeno L, Drumond A, Nieto R, Trigo RM, Stohl A (2010) On the origin of continental precipitation. Geophys Res Lett 37:L13804. doi:10.1029/2010GL043712

Arribas A, Glover M, Maidens A, Peterson K, Gordon M, MacLachlan C, Graham,R, Fereday D, Camp J, Scaife AA, Xavier P, McLean A, Colman A, Cusack S (2010) The GloSea4 ensemble prediction system for seasonal forecasting. Mon Weather Rev (in press)

Hewitt HT, Copsey D, Culverwell ID, Harris CM, Hill RSR, Keen AB, McLaren AJ, Hunke EC (2010) Design and implementation of the infrastructure of HadGEM3: the next-generation Met Office climate modelling system. Geosci Model Dev Discuss 3:1861–1937

Holton JR (1992) An introduction to dynamic meteorology, 3rd edn. Academic Press, San Diego

Hourdin F, Musat I, Bony S, Braconnot P, Codron F, Dufresne J-L, Fairhead L, Filiberti M-A, Friedlingstein P, Grandpeix J-Y, Krinner G, LeVan P, Li Z-X, Lott F (2006) The LMDZ4 general circulation model: climate performance and sensitivity to parametrized physics with emphasis on tropical convection. Clim Dyn 27:787–813. doi:10.1007/s00382-006-0158-0

Izumo T, de Boyer Montegut C, Luo JJ, Behera SK, Masson S, Yamagata T (2008) The role of the western Arabian Sea upwelling in Indian monsoon rainfall variability. J Clim 21:5603–5623. doi:10.1175/2008JCLI2158.1

Ju J, Slingo JM (1995) The Asian summer monsoon and ENSO. Q J R Meteorol Soc 121:1133–1168

Kim HJ, Wang B, Ding Q (2008) The global monsoon variability simulated by CMIP3 coupled climate models. J Clim 21:5271–5294. doi:10.1175/2008JCLI2041.1

Krishna Kumar K, Rajagopalan B, Cane MA (1999) On the weakening relationship between the Indian Monsoon and ENSO. Science 284(5423):2156–2159

Krishnan R, Swapna P (2009) Significant influence of the Boreal summer monsoon flow on the Indian Ocean response during dipole events. J Clim 22:5611–5634. doi:10.1175/2009JCLI2176.1

Krishnan R, Zhang C, Sugi M (2000) Dynamics of breaks in the Indian summer monsoon. J Atmos Sci 57:1354–1372. doi:10.1175/1520-0469

Kummerow C et al (2000) The status of the tropical rainfall measuring mission (TRMM) after two years in orbit. J Appl Meteorol 39:1965–1982. doi:10.1175/15200450(2001)040<1965:TSOTTR>2.0.CO;2

Li C, Yanai M (1996) The Onset and interannual variability of the Asian summer monsoon in relation to land–sea thermal contrast. J Clim 9:358–375. doi:10.1175/1520-0442

Lin JL (2007) The double-ITCZ problem in IPCC AR4 coupled GCMs: ocean–atmosphere feedback analysis. J Clim 20:4497–4525

Madec G (2008) NEMO ocean engine, Note du Pole de modélisation. Institut Pierre-Simon Laplace (IPSL) France 27. ISSN No 1288-1619

Martin GM, Ringer MA, Pope VD, Jones A, Dearden C, Hinton TJ (2006) The physical properties of the atmosphere in the New Hadley Centre global environmental model (HadGEM1). Part I: model description and global climatology. J Clim 19:1274–1301. doi:10.1175/JCLI3636.1

Martin GM, Milton SF, Senior CA, Brooks ME, Ineson S, Reichler T, Kim J (2010) Analysis and reduction of systematic errors through a seamless approach to modeling weather and climate. J Clim 23:5933–5957. doi:10.1175/2010JCLI3541.1

Meehl GA, Stocker TF, Collins WD, Friedlingstein P, Gaye AT, Gregory JM, Kitoh A, Knutti R, Murphy JM, Noda A, Raper SCB, Watterson IG, Weaver AJ, Zhao ZC (2007) Global climate projections. In: Solomon S, Qin D, Manning M, Chen Z, Marquis M, Averyt K, Tignor MMB, Miller HL (eds) Climate change 2007: the physical science basis. Contribution of working group I to the fourth assessment report of the intergovernmental panel on climate. Cambridge University Press, Cambridge

Neale R, Slingo J (2003) The maritime continent and its role in the global climate: a GCM study. J Clim 16:834–848. doi:10.1175/1520-0442(2003)016<0834:TMCAIR>2.0.CO;2

Parthasarathy B, Munot AA, Kothwale SR (1995) Monthly and seasonal rainfall series for all-India homogeneous regions and meteorological subdivisions: 1871–1994. Contributions from Indian Institute of Tropical Meteorology, Pune-411 008, India

Rajeevan M, Nanjundiah RS (2009) Coupled model simulations of twentieth century climate of the Indian summer monsoon. Current trends in science, platinum jubilee special volume of the Indian Academy of Sciences. Indian Academy of Science, Bangalore, pp 537–568. Available at http://www.ias.ac.in

Rajeevan M, Bhate J, Kale JD, Lal B (2006) High resolution daily gridded rainfall data for the Indian region: analysis of break and active monsoon spells. Curr Sci 91:296–306

Rao KG, Goswami BN (1988) Interannual variations of SST over the Arabian Sea and the Indian monsoon: a new perspective. Mon Weather Rev 116:558–568

Rayner NA, Parker DE, Horton EB, Folland CK, Alexander LV, Rowell DP, Kent EC, Kaplan A (2003) Global analyses of sea surface temperature, sea ice, and night marine air temperature since the late nineteenth century. J Geophys Res 108(D14):4407–4435. doi:10.1029/2002JD002670

Rayner NA, Brohan P, Parker DE, Folland CK, Kennedy JJ, Vanicek M, Ansell T, Tett SFB (2006) Improved analyses of changes and uncertainties in sea surface temperature measured in situ since the mid-nineteenth century: the HadSST2 data set. J Clim 19(3):446–469. doi:10.1175/JCLI3637.1

Reynolds RWT, Smith M, Liu C, Chelton DB, Casey KS, Schlax MG (2007) Daily high-resolution blended analyses for sea surface temperature. J Clim 20:5473–5496. doi:10.1175/2007JCLI1824.1

Saji NH, Goswami BN, Vinayachandran PN, Yamagata T (1999) A dipole mode in the tropical Indian Ocean. Nature 401:360–363

Shaffrey LC, Stevens IG, Norton WA, Roberts MJ, Vidale PL, Harle JD, Jrrar A, Stevens DP, Woodage MJ, Demory ME, Donners J, Clark DB, Clayton A, Cole JW, King JC, New AL, Slingo JM, Slingo A, Steenman-Clark L, Martin GM (2009) UK-HiGEM: the new UK high resolution global environment model. Model description and basic evaluation. J Clim 22:1861–1896. doi:10.1175/2008JCLI2508.1

Shukla J (1975) Effect of Arabian Sea-surface temperature anomaly on Indian summer monsoon: a numerical experiment with the GFDL model. J Atmos Sci 32(3):503–511

Singh GP, Oh JH (2007) Impact of Indian Ocean sea-surface temperature anomaly on Indian summer monsoon precipitation using a regional climate model. Int J Climatol 27:1455–1465. doi:10.1002/joc.1485

Soman MK, Slingo JM (1997) Sensitivity of the Asian summer monsoon to aspects of sea-surface temperature anomalies in the tropical Pacific Ocean. Q J R Meteorol Soc 123:309–336

Sperber KR, Slingo JM, Annamalai H (2000) Predictability and the relationship between subseasonal and interannual variability during the Asian summer monsoon. Q J R Meteorol Soc 126:2514–2545

Strachan J (2007) Understanding and modelling the climate of the maritime continent. PhD dissertation, University of Reading

Taylor KE, Williamson D, Zwiers F (2000) The sea surface temperature and sea-ice concentration boundary conditions for AMIP II simulations. PCMDI Report 60, Program for climate model diagnosis and intercomparison, Lawrence Livermore National Laboratory, Livermore, California

Turner AG, Inness PM, Slingo JM (2005) The role of the basic state in the ENSO-Monsoon relationship and implications for predictability. Q J R Meteorol Soc 131(607):781–804. doi:10.1256/qj.04.70

Uppala SM, KÅllberg PW, Simmons AJ, Andrae U, Bechtold VDC, Fiorino M, Gibson JK, Haseler J, Hernandez A, Kelly GA, Li X, Onogi K, Saarinen S, Sokka N, Allan RP, Andersson E, Arpe K, Balmaseda MA, Beljaars ACM, Berg LVD, Bidlot J, Bormann N, Caires S, Chevallier F, Dethof A, Dragosavac M, Fisher M, Fuentes M, Hagemann S, Hólm E, Hoskins BJ, Isaksen L, Janssen PAEM, Jenne R, Mcnally AP, Mahfouf JF, Morcrette JJ, Rayner NA, Saunders RW, Simon P, Sterl A, Trenberth KE, Untch A, Vasiljevic D, Viterbo P, Woollen J (2005) The ERA-40 re-analysis. Q J R Meteorol Soc 131:2961–3012. doi:10.1256/qj.04.176

Oldenborgh GJ van, Burgers G (2005) Searching for decadal variations in ENSO precipitation teleconnections. Geophys Res Lett 32(15):L15701. doi:10.1029/2005GL023110

Vecchi GA, Harrison DE (2004) Interannual Indian rainfall variability and Indian Ocean Sea surface temperature anomalies. In: Wang C, Xie SP, Carton JA (eds) Earth climate: the ocean–atmosphere interaction. American Geophysical Union, Geophysical Monograph 147, Washington DC, pp 247–260

Walker GT (1925) Correlation in seasonal variations of weather—a further study of world weather. Mon Wea Rev 53(6):252–254. doi:10.1175/1520-0493(1925)53<252:cisvow>2.0co;2

Washington WM, Chervin RM, Rao GV (1977) Effects of a variety of Indian Ocean surface temperature anomaly patterns on the summer monsoon circulation: experiments with the NCAR general circulation model. Pure Appl Geophys 115:1335–1356

Webster PJ, Yang S (1992) Monsoon and ENSO: selectively interactive systems. Q J R Meteorol Soc 118:877–926

Webster PJ, Moore AM, Loschnigg JP, Leben RR (1999) Coupled ocean–atmosphere dynamics in the Indian Ocean during 1997–98. Nature 401:356–360

Wilson DR, Bushell AC, Kerr-Munslow AM, Price JD, Morcrette CJ (2008) PC2: a prognostic cloud fraction and condensation scheme I: scheme description. Q J R Meteorol Soc 134:2093–2107. doi:10.1002/qj.333

Xie P, Arkin PA (1996) Analysis of global monthly precipitation using gauge observations, satellite estimates, and numerical model predictions. J Clim 9:840–858